

Original Article

Cite this article: Seybold L, Dörr W, Trepmann CA, and Krahl J (2020) New constraints from U–Pb dating of detrital zircons on the palaeogeographic origin of metasediments in the Talea Ori, central Crete. *Geological Magazine* **157**: 1383–1408. <https://doi.org/10.1017/S0016756819001365>

Received: 22 May 2019

Revised: 17 September 2019

Accepted: 19 October 2019

First published online: 13 January 2020

Keywords:

External Hellenides; Sakarya Zone; HP-LT; Plattenkalk unit; Phyllite–Quartzite unit; tectonics; Eastern Mediterranean

Author for correspondence:

Lina Seybold, Email: lina.seybold@lmu.de

New constraints from U–Pb dating of detrital zircons on the palaeogeographic origin of metasediments in the Talea Ori, central Crete

Lina Seybold¹ , Wolfgang Dörr², Claudia A. Trepmann¹ and Jochen Krahl³

¹Ludwig-Maximilians-Universität, Luisenstraße 37, 80333 Munich, Germany; ²Institut für Geowissenschaften, Universität Frankfurt a.M., Altenhöferallee 1, 60438 Frankfurt, Germany and ³Agnesstraße 45, 80798 Munich, Germany

Abstract

High-pressure low-temperature metamorphic sediments of the Phyllite–Quartzite unit *sensu stricto* and the Talea Ori group are investigated in the field, microstructurally and by U–Pb dating of detrital zircons to shed light on their palaeogeographic origin. Zircon age spectra with ages >450 Ma of the Phyllite–Quartzite unit *sensu stricto* indicate a palaeogeographic origin at the northern margin of East Gondwana. In contrast, the lower stratigraphic, siliciclastic formations of the Talea Ori group show a high number of well-rounded Cambrian to Early Carboniferous aged zircons and a Neoproterozoic zircon age spectrum with East Gondwana affinity. Based on the comparison of zircon age data, a possible distal sediment source is the Sakarya Zone at the southern active margin of Eurasia. To reconcile the zircon data with the geological observations we propose different alternative models, or a combination of these, including sediment transport from the Sakarya Zone and/or a westerly source towards the northern margin of Gondwana as well as terrane-displacement of the Sakarya Zone. Also, a palaeogeographic origin of the Talea Ori group at the southern active margin of Eurasia cannot be excluded. This alternative, however, would not be consistent with the usually assumed association of the Talea Ori group with the Plattenkalk unit characterized by a palaeogeographic origin at the northern margin of Gondwana.

1. Introduction

The Talea Ori group in central Crete comprises platy marbles with chert in its stratigraphic top (e.g. Epting *et al.* 1972; Kuss & Thorbecke, 1974; Hall & Audley-Charles, 1983; Krahl *et al.* 1988) and structurally underlies the Phyllite–Quartzite unit *sensu stricto* (Zulauf *et al.* 2016; Seybold *et al.* 2019). Because of the similarities in lithofacies and structural position, the Talea Ori group is associated with the ‘paraautochthonous’ Plattenkalk unit cropping out e.g. in the Ida Ori and Lefka Ori on Crete (e.g. Creutzburg & Seidel, 1975; Hall & Audley-Charles, 1983; Bonneau, 1984; Jacobshagen *et al.* 1986). Yet, the Talea Ori group underwent high-pressure low-temperature (HP-LT) metamorphism and therefore must be allochthonous (Seidel, 1978; Seidel *et al.* 1982; Theye, 1988; Theye *et al.* 1992). The Plattenkalk unit is considered the most external and lowermost unit of the Hellenides, and its basement is not exposed (e.g. Hall & Audley-Charles, 1983; Bonneau, 1984; Jacobshagen *et al.* 1986; Krahl *et al.* 1988). The stratigraphic base of the Talea Ori group, a siliciclastic/carbonatic metamorphic sequence, is not known from any other exposures of the Plattenkalk unit on Crete and the Peloponnesus (e.g. Creutzburg & Seidel, 1975; Jacobshagen *et al.* 1978, 1986; Bonneau, 1984; Manutsoglu *et al.* 1995a; Soujon *et al.* 1998; Kock *et al.* 2007). Given the fact that in the Talea Ori the HP-LT metamorphic lowermost units of the Cretan nappe pile are exclusively exposed, it has been the subject of several petrological and structural studies to unravel the Alpine subduction and exhumation history (e.g. Seidel *et al.* 1982; Richter & Kopp, 1983; Theye, 1988; Seybold *et al.* 2019; Trepmann & Seybold, 2019). Furthermore, the Talea Ori is a key area for unravelling the palaeogeographic relationships and the large-scale tectonic development of the Eastern Mediterranean (e.g. Stampfli *et al.* 2003; Robertson, 2006; Kock *et al.* 2007; Zulauf *et al.* 2018). There are several alternative tectonic models discussed e.g. by Robertson (2006), including northward subduction, southward subduction and double subduction, in which the Talea Ori group and Plattenkalk unit restore either to a position at the northern margin of Gondwana (Dornsiepen *et al.* 2001; Robertson, 2006, 2012) or to the southern margin of the ‘Cimmerian’ continent (Stampfli & Borel, 2002; Kock *et al.* 2007; Stampfli *et al.* 2013). The Cimmerian blocks started drifting northwards from Gondwana in Late Carboniferous to Early Permian times and collided with the southern Eurasian margin during the Eo-Cimmerian events in Middle Triassic times (Stampfli & Borel, 2002). According to Zulauf *et al.* (2018), the Plattenkalk unit restores to the northern margin of Gondwana.

© Cambridge University Press 2020. This is an Open Access article, distributed under the terms of the Creative Commons Attribution licence (<http://creativecommons.org/licenses/by/4.0/>), which permits unrestricted re-use, distribution, and reproduction in any medium, provided the original work is properly cited.

CAMBRIDGE
UNIVERSITY PRESS

Within the Cretan nappe pile, the Plattenkalk unit is structurally overlain by the Phyllite–Quartzite unit *sensu lato* (PQ s.l.), comprising the Trypali unit, the Phyllite–Quartzite unit *sensu stricto* (PQ s.str.), a pre-Alpine basement unit and the Tyros unit (Dornsiepen & Manutsoglu, 1994; Zulauf *et al.* 2008). The palaeogeographic origin of the PQ s.str. is generally considered at the northern margin of Gondwana to the north of the Plattenkalk unit and Talea Ori group (e.g. Kozur & Krahl, 1987; Baud *et al.* 1993; Marcoux & Baud, 1995; Dornsiepen *et al.* 2001; Stampfli *et al.* 2003; Robertson, 2006, 2012; Stampfli & Kozur, 2006).

Detrital zircon dating was carried out on several outcrops of the PQ s.l. on Crete and the Peloponnesus (Dörr *et al.* 2015; Zulauf *et al.* 2015; Chatzaras *et al.* 2016; Zulauf *et al.* 2018) and the Talea Ori group in central Crete (Kock *et al.* 2007; Zulauf *et al.* 2016). A large amount of Variscan-aged zircons was reported from the metasandstones at the stratigraphic base of the Talea Ori group (Bali formation; Seybold *et al.* 2019), in contrast to detrital zircons from the PQ s.str., which systematically do not show Variscan ages (Zulauf *et al.* 2016). These findings challenge the interpretation that the Talea Ori group can be associated with the Plattenkalk unit and deposited at the northern margin of Gondwana (Dornsiepen *et al.* 2001) or Cimmeria (Stampfli *et al.* 2003; Kock *et al.* 2007; Moix *et al.* 2008). Therefore, Zulauf *et al.* (2016) suggested that the metasediments of the Bali formation were deposited at the active convergent margin of southern Eurasia, where the Palaeotethys was subducted beneath Eurasia in Permo-Triassic times. In contrast, Kock *et al.* (2007) proposed that Variscan detritus was transported to the Bali formation, which deposited in the rift between Gondwana and Cimmeria, by a river system from the Variscan belt in the west that was active during the Carboniferous. As a large amount of the zircons of the Bali formation are euhedral (Kock *et al.* 2007; Zulauf *et al.* 2016), long-distance transport of the zircons is, however, ambiguous.

In this study, we present new U–Pb ages of detrital zircons from the siliciclastic/carbonatic Upper Carboniferous / Lower Permian to Olenekian formations of the lower Talea Ori group (Fig. 1) and the structurally overlying PQ s.str. and we analyse components of metaconglomerates at the base of the Talea Ori group. The palaeogeographic origin of the Talea Ori group and its association with the Plattenkalk unit are discussed, taking zircon data, lithofacies and structural viewpoints into account.

2. Regional geology

The External Hellenides comprise several tectonic nappes that were stacked during the Alpine mountain building (Fig. 1). The lower nappes, including parts of the PQ s.l., the Talea Ori group and the Plattenkalk unit, experienced HP–LT metamorphism during subduction in Late Oligocene to Miocene times and were rapidly exhumed (e.g. Seidel *et al.* 1982, 2007; Thomson *et al.* 1998, 1999; Deckert *et al.* 1999). In the Talea Ori in central Crete, HP–LT metamorphic rocks of the Talea Ori group are structurally overlain by the PQ s.str. (Fig. 1; Zulauf *et al.* 2016; Seybold *et al.* 2019). The Talea Ori group is structurally inverted, with the southern carbonate-dominated units forming the overturned limb of a large-scale south-vergent fold structure with eastward-plunging fold axis (Fig. 1; Epting *et al.* 1972; König & Kuss 1980; Hall & Audley-Charles, 1983; Richter & Kopp, 1983; Krahl *et al.* 1988; Chatzaras *et al.* 2006; Robertson, 2006; Kock *et al.* 2007; Seybold *et al.* 2019). The stratigraphic contacts are often overprinted by younger normal faults, but the regular dipping of the layering and an at least locally still assessable sedimentary nature of the

contacts indicates the stratigraphic relation of the different formations (e.g. Epting *et al.* 1972; Richter & Kopp, 1983; Kock *et al.* 2007).

The stratigraphic base of the Talea Ori group is formed by the Bali formation (also addressed as Galinos beds (Kock *et al.* 2007; König & Kuss, 1980), or as lower Fodele formation (Richter & Kopp, 1983)), a mainly siliciclastic alternation of metasandstones, black metacherts, quartz-metaconglomerates and black shales (Fig. 1c, d; Seybold *et al.* 2019). The age of the Bali formation has been determined by König & Kuss (1980) to be Late Carboniferous / Early Permian, based on a fauna of macrofossils including brachiopods, trilobites and goniatites. Exclusively at the beach of Bali village, marbles also occur within the Bali formation, which are interpreted as shallow water patch reefs (König & Kuss, 1980; Kock *et al.* 2007). The Bali formation is stratigraphically overlain by the Fodele formation (Fig. 1d), characterized by 400–600 m thick dark dolomitic fossil-rich marbles (e.g. fusulinids, bryozoans, brachiopods, coral fragments), which in the lower part alternate with metasandstones and black shales (Epting *et al.* 1972). According to corals, fusulinids and bryozoans, the Fodele formation is of Middle to Late Permian age (Kuss, 1963, 1973; Epting *et al.* 1972; Kuss & Thorbecke, 1974; König & Kuss, 1980). The stratigraphically overlying Sisses formation (Epting *et al.* 1972; König & Kuss 1980) comprises greenish to violet phyllites, light metasandstones, light fine-grained dolomite marbles and carbonatic metaconglomerates. An Olenekian age has been determined for the dolomite marbles (conodonts; König & Kuss, 1980). The Bali, Fodele and Sisses formations are grouped in this study as the lower Talea Ori group (Fig. 1d). The contact to the stratigraphically overlying upper formations of the Talea Ori group (upper Talea Ori group; Fig. 1d) is erosive with palaeokarst filled by metabauxite (Epting *et al.* 1972; Kock *et al.* 2007), indicating tectonic uplift (Stampfli *et al.* 2003; Robertson, 2006) before deposition of the Norian to Liassic Mavri formation (foraminifers (Epting *et al.* 1972); dasycladaceae (Krahl *et al.* 1988; Soujon *et al.* 1998)). The latter are characterized by stromatolitic dolomite marble (Epting *et al.* 1972; Krahl *et al.* 1988; Kock *et al.* 2007). The stratigraphic top of the Talea Ori group is formed by the Aloides formation (Epting *et al.* 1972; Hall & Audley-Charles, 1983; Krahl *et al.* 1988; Soujon *et al.* 1998; Krahl & Kauffmann 2004), a sequence of platy marbles with chert comprising coarse carbonate breccias at the base. In their upper part, layers of greenish phyllite occur (Gigilos beds; Katsivrias *et al.* 2008) and pelagic platy marbles with chert nodules or layers (Plattenkalk (Epting *et al.* 1972; Hall & Audley-Charles, 1983)). Fossils, which are relevant for dating, are rare in the formation, but cephalopods indicate an Early Jurassic age in the lower stratigraphic beds of the formation (Kuss, 1982; Krahl *et al.* 1988). The rock strata of the Plattenkalk unit exposed in several different outcrops on Crete are of Jurassic to Eocene age (foraminifers, east Crete (Fytrolakis 1972), rudists, east Crete (Wachendorf *et al.* 1980); nummulites, Lefka Ori (Alexopoulos *et al.* 2000)), but in the Talea Ori the youngest member of the Plattenkalk unit, the Eocene Kalavros beds cropping out e.g. in the Ida Ori to the south, is missing (Fytrolakis 1972; Krahl *et al.* 1988). The siliciclastic/carbonatic succession of the lower Talea Ori group (Bali, Fodele and Sisses formations) is not known from any other outcrop of the Plattenkalk unit on Crete. In the Taygetos mountains, Peloponnesus, the Plattenkalk is underlain by the Kastania phyllites, but a correlation with the Talea Ori group is equivocal because the Kastania phyllites are mainly siliciclastic, containing only thin layers of carbonates (Kowalczyk & Dittmar, 1991), and are rather similar to the phyllites and quartzites of western Crete (Robertson, 2006).

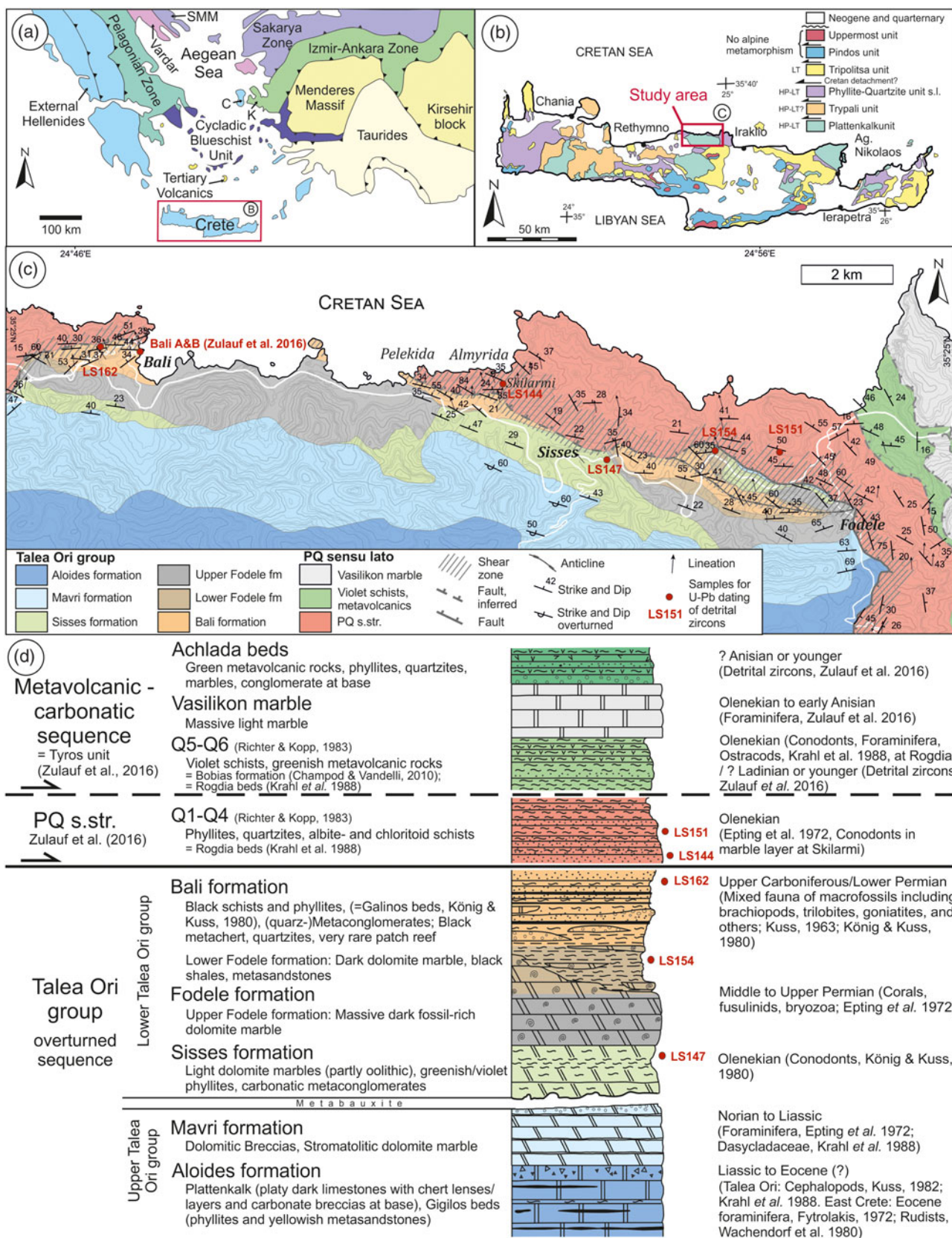


Fig. 1. Geologic map of (a) the Eastern Mediterranean, modified after Zulauf *et al.* (2007), abbreviations: C = Chios, K = Karaburun; (b) the island of Crete, modified after Creutzburg & Seidel (1975); and (c) the Talea Ori, central Crete, modified after Epting *et al.* (1972). The structural data and location of the shear zone are based on Seybold *et al.* (2019). (d) Stratigraphic column of the different tectonostratigraphic units cropping out in the Talea Ori, modified after Epting *et al.* (1972). The given ages are biostratigraphic ages based on the macro- and microfossil records of the rocks.

The PQ s.str. in the Talea Ori (Zulauf *et al.* 2016) shows a detrital zircon age pattern that is in accordance with the PQ s.str. in eastern and western Crete and the Peloponnesus, with zircon ages being typically older than ~450 Ma (Chatzaras *et al.* 2016). Known biostratigraphic ages of the PQ s.str. in western and eastern Crete are Late Carboniferous to Late Triassic (Krahl *et al.* 1983, 1986; Kozur & Krahl, 1987; Zulauf *et al.* 2018). The sedimentation age of the PQ s.str. in the Talea Ori is uncertain, because one biostratigraphic age, determined by Epting *et al.* (1972) to be Olenekian, stems from a marble which some authors interpret as belonging to the Sisses formation of the Talea Ori group (e.g. Kuss & Thorbecke, 1974; Richter & Kopp, 1983). A conodont *Hindeodus parvus* (Kozur & Pjatakova, 1976), of the Permian–Triassic boundary was found at the southern border of the Talea Ori.

The PQ s.str. in the eastern Talea Ori is overlain by an association of violet schists, greenish metavolcanic rocks and carbonatic rocks (Fig. 1d), that was variously named Q5–Q6 (Richter & Kopp, 1983), Rogdia beds (Krahl *et al.* 1988), Bobias formation (Champod & Vandelli, 2010) and upper Rogdia beds (Zulauf *et al.* 2016). The fossil record of samples in this metavolcanic/carbonatic sequence as well as in an overlying marble – the Vasilikon marble – gives Olenekian/Anisian sedimentation ages (Krahl *et al.* 1988; Champod & Vandelli, 2010; Zulauf *et al.* 2016). Zulauf *et al.* (2016) attributed the metavolcanic/carbonatic sequence to the ‘Tyros unit’ of eastern Crete (Zulauf *et al.* 2008). The detrital zircon patterns of this unit are characterized by a high amount of Variscan-aged zircons and are similar to the zircon spectra of the Bali formation (Zulauf *et al.* 2016). Because of this similarity, Zulauf *et al.* (2016) inferred that the Bali formation and upper Rogdia beds can be associated with the Tyros unit of eastern Crete and deposited on the southern active margin of Eurasia. In eastern Crete, the Tyros unit is located above a pre-Alpine basement unit that is thrust upon the PQ s.str. (Zulauf *et al.* 2008; Klein *et al.* 2013).

Characteristic mineral assemblages comprising e.g. Mg-carpholite, sudoite, chloritoid, topaz and lawsonite in the Sisses formation and blue amphibole (crossite) in the metavolcanic rocks indicate that all units, cropping out in the Talea Ori, experienced Alpine *P–T* conditions of ~0.9 GPa and ~350 °C, thus indicating subduction to ~30 km depth (Seidel, 1978; Seidel *et al.* 1982; Theye, 1988; Theye & Seidel, 1991; Theye *et al.* 1992). The temperature constraints are consistent with the degree of graphitization of carbonaceous material for central Crete (Rahl *et al.* 2005; Seybold *et al.* 2019). The tectonic contact between the Talea Ori group and the PQ s.str. was commonly described as thrust fault, according to the general nappe character of the Talea Ori group and the PQ s.str. (e.g. Chatzaras *et al.* 2006; Xypolias *et al.*, 2007) although a normal character of the contact was recognized already by Richter & Kopp (1983). The Talea Ori group and the PQ s.str. were juxtaposed already at peak metamorphic temperatures and experienced a similar tectonometamorphic history (e.g. Thomson *et al.* 1999), with the latest ductile deformation being localized in an extensional shear zone due to updoming and exhumation of the HP-LT metamorphic rocks (Seybold *et al.* 2019).

3. Analytical methods

Structural and lithological mapping in the northern area of the Talea Ori (Fig. 1) was carried out in field trips between 2016

and 2018. Samples from characteristic outcrops of the siliciclastic units were taken, and standard petrographic thin-sections (30 µm thickness) were prepared for microstructural characterization of the metasediments using polarized light microscopy. The thin-sections were prepared perpendicular to the foliation and parallel to the stretching lineation, if present. U–Pb dating was performed on detrital zircons of five metasediments and quartzites of the Bali (LS162), Fodele (LS154) and Sisses (LS147) formations as well as the PQ s.str. (LS144, LS151). For analysis by laser ablation inductively coupled plasma mass spectrometry (LA-ICPMS), samples were processed at the Institut für Geowissenschaften of the Goethe University, Frankfurt Main, using standard mineral-separation techniques. These include crushing by hammer and grinding in a disc mill, followed by concentration of the heavy mineral fraction by wet shaking table, heavy liquids (bromoform, methylenediodide) and magnetic separation with a Frantz isodynamic separator.

Hand-picked zircon grains were mounted in 25 mm diameter circular epoxy mounts and polished to expose a section at their inner core. Before and after LA-ICP-MS analysis, the grains were examined using cathodoluminescence (CL) imaging in order to recognize their internal structure and to identify cracks and mineral inclusions. Zircon U–Pb isotope analysis was performed by LA-ICP-MS technique using a Thermo-Finnigan Element II sector field ICPMS attached to a New Wave LUV213 laser ablation system ($\lambda = 213$ nm). Ablation was carried out in a He carrier gas in a low-volume (2.5 cm³) cell; laser beam parameters used were 30 µm diameter; 5 Hz repetition rate 75 % power output. Isotope data were acquired in peak-jumping mode on eight masses: ²⁰²Hg, ²⁰⁴Pb, ²⁰⁶Pb, ²⁰⁷Pb, ²⁰⁸Pb, ²³⁵U and ²³⁸U. Background and ablation data for each analysis were collected over 90 s, with background measurements (carrier gas, no ablation) being taken over the first 30 s prior to initiation of ablation. Data were collected at time-resolved mode allowing acquisition of the signal as a function of time (ablation depth), and subsequently recognition of isotopic heterogeneities within the ablated volume. Raw data were processed offline using an Excel® spreadsheet program (Frei & Gerdes, 2009). Mass discrimination of the MS, and elemental fractionation during laser ablation were corrected by calibration against the GJ-1 zircon standard (Jackson *et al.* 2004), which was analysed routinely during analytical sessions (three standard analyses at the beginning and end of every session of 33 unknowns, and two standard analyses every 10 unknowns). Prior to this correction, the change of elemental fractionation (e.g. Pb/U and Pb/Th ratios as function of ablation time and thus depth) was corrected for each set of isotope ratios by applying a linear regression through all measured ratios versus time, excluding some outliers (>2 s.e.), and taking the intercept $t = 0$ as the correct ratio. Changes in isotopic ratios arising from laser drilling into domains of distinct Pb/U ratio (core/rim), mineral inclusions, and zones affected by Pb loss (metamictization/cracks), can usually be detected by careful monitoring of the time-resolved signal; such analyses are normally rejected. Common Pb correction was applied only when the interference- and background-corrected ²⁰⁴Pb signal was significantly higher than the detection limit of *c.* 20 cps. The latter is limited by the amount of Hg in the carrier gas and the accuracy to which the ²⁰²Hg and thus the interfering ²⁰⁴Hg can be monitored. Corrections made were based on common Pb composition given by the two-stage growth curve of Stacey & Kramers (1975). In order to monitor the reproducibility and accuracy of our analytical

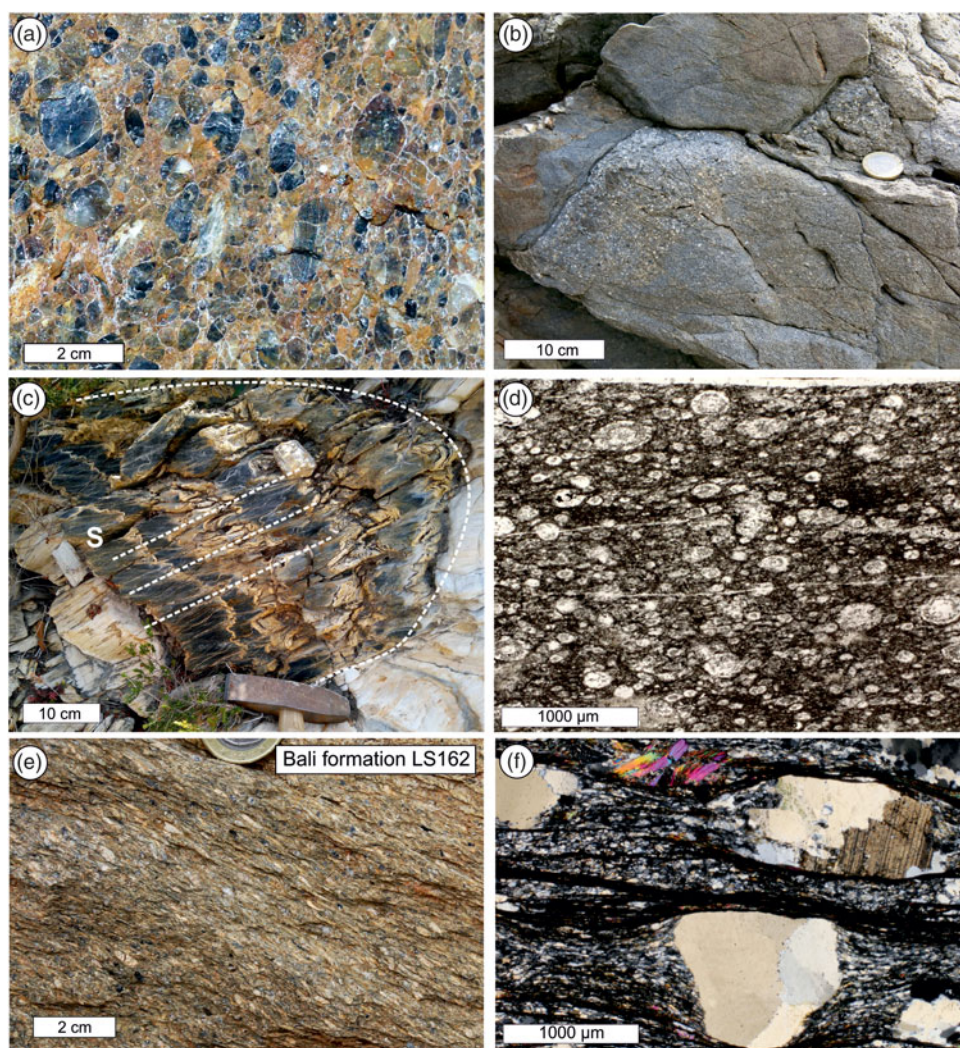


Fig. 2. Bali formation at the stratigraphic base of the Talea Ori group. (a) Quartz metaconglomerate with >90% black vein quartz pebbles (Bali beach). (b) Inverted graded bedding in metasandstones associated with the quartz metaconglomerate, south of the port of Bali. (c) Folded black metachert/shale interlayering with axial plane foliation, west of Galinos. (d) Metachert with fossil relics (LS75, Bali beach). (e, f) Coarse-grained metasandstone sampled for U–Pb dating of detrital zircons (LS162, NW of Bali) (photomicrograph in (f) taken with crossed polarizers).

procedure, the standard zircon 91500 (Wiedenbeck *et al.* 1995) has been reproduced with an age of 1063 ± 3 Ma.

4. Results

The U–Pb results obtained from the metasedimentary rocks are presented on density / relative probability plots (Ludwig, 2001) with a concordance ($^{207}\text{Pb}/^{206}\text{Pb}$ age / $^{206}\text{Pb}/^{238}\text{U}$ age * 100) from 90 to 110%. To present the whole age spectrum of detrital zircons of a sample they were plotted with their $^{207}\text{Pb}/^{206}\text{Pb}$ ages. For a better comparison of the zircons younger than 1.1 Ga, they were plotted with their $^{206}\text{Pb}/^{238}\text{U}$ ages in a separate diagram. The relative probability plot of Ludwig (2001) was used, because it takes the analytical uncertainties into account. If not stated elsewhere, the age peaks are calculated with the concordant analyses (97 to 103% concordance) as concordia age of a zircon population defined by Ludwig (2001). In most cases, the oscillatory-zoned parts between the core and rim of the zircons are measured, because these parts reflect the undisturbed zircon growth and thus an undisturbed U–Pb system of the zircons with no or minor lead loss. For tables of the zircon data and concordia ages refer to the online Supplementary Material at <http://journals.cambridge.org/geo>. There, also, cross-sections of the Talea Ori with indicated sample positions are shown (Supplementary Figure S6). Lithologic and U–Pb analyses of detrital zircons are described for each sample in the following sections.

4.a. Bali formation

The stratigraphic base of the Talea Ori group was formerly variously named, associated and mapped (e.g. Talea Ori phyllite (Epting *et al.* 1972); Galinos shale (König & Kuss, 1980); lower Fodele formation (Richter & Kopp, 1983)), given the similar appearance of the strongly deformed metasediments in the shear zone at the contact to the PQ s.str. (Seybold *et al.* 2019). Here, we present a detailed description and a new coherent mapping of the outcrops of the Bali formation in the Talea Ori (Fig. 1a).

4.a.1. Lithologies of the Bali formation

The formation includes interlayered black shales (named Galinos shale by König & Kuss, 1980), metasandstones, (quartz-) metaconglomerates (Fig. 2a; Trepmann *et al.* 2010), black quartzites, black metachert and locally fossil-rich calcitic marbles. The type location of the formation is the bay of Bali where the complete sequence of lithologies is exposed (Fig. 1). In particular, the quartz-metacglomerates and metacherts are the characteristic lithologies of the formation and were found at several new outcrops also to the east of Bali village (Seybold *et al.* 2019). At the bay of Bali, graded bedding coarsening upwards can be observed (Fig. 2b) locally in metasandstones, which is consistent with an overturned layering of the Talea Ori group (e.g. Epting *et al.* 1972). The metacherts (Fig. 2c, d) and the black shales occur as several-metre-thick

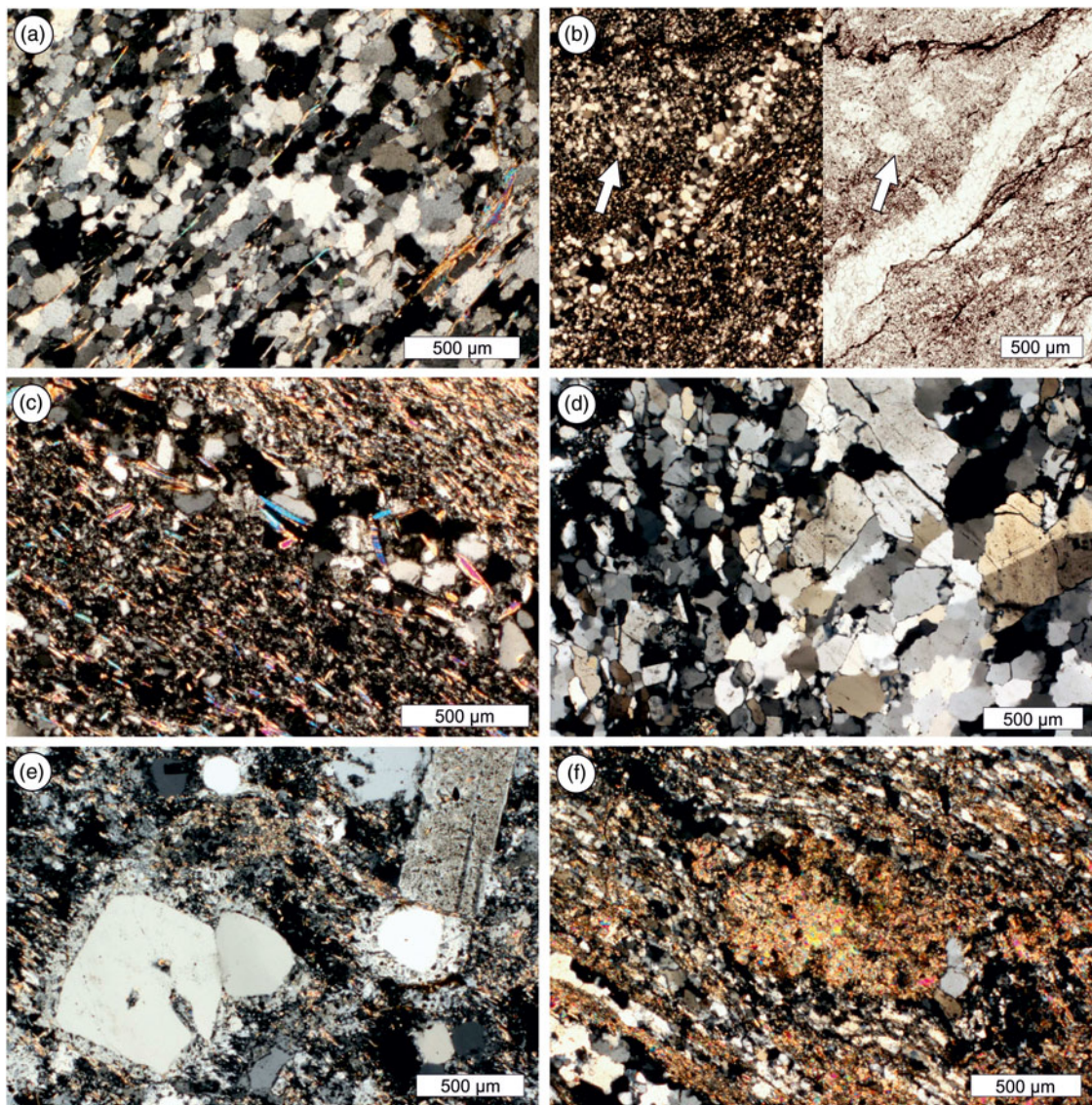


Fig. 3. Photomicrographs of the components of the Bali quartz-metaconglomerate and metasandstones. (a) Quartzite with mica flakes (crossed polarizers CT785). (b) Metachert with coarser quartz veins and ellipsoidal components visible mainly with plane polarized light (white arrows) (CT785i, left: crossed polarizers, right: plane polarizers). (c) Metapelite with psammitic layer (LS70 crossed polarizers). (d) Albite–quartz aggregates; here also the finer-grained matrix largely consists of small isometric grains of albite (LS261G crossed polarizers). (e) Felsic volcanic rock (LS261A crossed polarizers): euhedral quartz with resorption embayments and plagioclase with sericitization in fine-grained quartz–plagioclase–sericite matrix; quartz shows overgrowth rims. (f) Retrograde mica schist with aggregate of fine-grained phyllosilicates (LS261F crossed polarizers).

layers and as coarse intraformational metaconglomerates/breccias in the formation. The black shales can also contain black quartz-pebbles, comparable to vein quartz pebbles in the quartz metaconglomerates. Locally, microfossils (radiolarians, ostracods) are preserved in the metachert, which are visible in thin-section with reflected light (Fig. 2d, 3b); radiolarians are already mentioned by Kock *et al.* (2007). The metaconglomerates, metasandstones and shales compose a turbiditic sequence with strongly varying proportions of shale, chert and vein quartz components. The Bali quartz-metaconglomerate represents a quartz-component-rich end-member. Metasandstones are increasingly prominent towards the contact to the PQ s.str., where they vary from mica-rich metasandstones containing up to ~6 % feldspar to black quartzites. The feldspar as well as the mica in the metasandstones and in the quartz metaconglomerate are partly of detrital nature, but also metamorphic mica and albite porphyroblasts occur, the latter revealing

aligned inclusions of white mica, biotite, quartz, graphite and rutile that form an internal foliation (Seybold *et al.* 2019). Such albite blasts are also present in the Sisses formation and they typically occur in albite schists of the PQ s.str. (Zulauf *et al.* 2016; Seybold *et al.* 2019).

4.a.2. *Clast lithologies of the Bali quartz metaconglomerate*

The Bali quartz metaconglomerate contains mm- to several cm-large well-rounded pebbles of different lithologies (Figs 2a, e, f, 3). The most frequent rock type is the black well-rounded quartz pebbles, derived from quartz veins (Fig. 2a, f; Trepmann *et al.* 2010). In the different layers of the metaconglomerate, the proportion of vein quartz clasts to lithic clasts varies between 100–80 % vein quartz and 0–20 % lithic clasts.

Seven different rock types occur as clasts: vein quartz (Fig. 2a, f), quartzite (Fig. 3a), chert (Fig. 3b), pelitic/psammitic siliciclastic

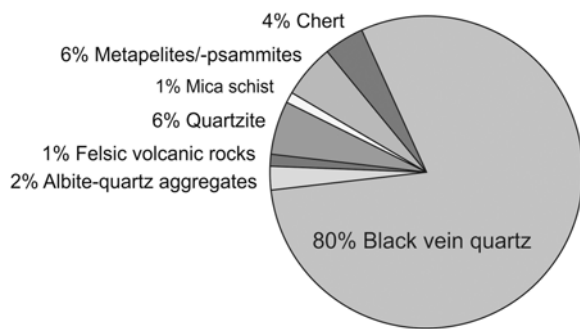


Fig. 4. Abundance of different pebbles of the Bali quartz metaconglomerate.

(meta-) sedimentary rocks (Fig. 3c), albite–quartz aggregates (Figs 2d, 3d), felsic volcanic rocks (Fig. 3e) and mica schists (Fig. 3f). The abundance of the different pebbles is shown in Figure 4. Whereas the metacherts and pelitic/psammitic metasediments crop out in the Talea Ori in close association with the Bali quartz–metaconglomerate, felsic volcanic rocks as well as the black vein quartz are not exposed anywhere in the Talea Ori.

The quartzite pebbles usually show an internal foliation characterized by the shape preferred orientation of quartz and mica (Fig. 3a). Pebbles originating from chert comprise foliated fine-grained quartz layers without crystallographic preferred orientation of the isometric quartz grains and dispersed opaque phases, which are commonly cross-cut by coarser quartz veins (Fig. 3b). Pebbles containing aggregates of coarse-grained quartz and twinned albite are interpreted to be derived from hydrothermal albite–quartz veins (Fig. 3d) that similarly occur in the PQ s.str.; however, an igneous source is also possible (Fig. 2f). Rare fine-grained light pebbles with up to dm size comprise euhedral plagioclase with sericitization, quartz phenocrysts with embayments and a low amount of K-feldspar in a fine-grained sericite–quartz matrix (Fig. 3e). The source rock of these components is interpreted as volcanic rock of probably dacitic or rhyolitic composition. Foliated quartz- and mica-rich components can contain aggregates of fine-grained phyllosilicates replacing former minerals (Fig. 3f). These mica-rich components as well as single detrital mica grains are interpreted to be derived from mica schists (Fig. 2f).

4.a.3. Coarse-grained metasandstone (LS162)

For U–Pb dating of detrital zircons, a foliated, coarse-grained metasandstone with elongate quartz clasts and lithic clasts of typically about several mm length and several hundreds of μm width (Fig. 2e, f) was sampled from the Bali formation west of Bali village close to the contact to the PQ s.str. (LS162, Fig. 1; $35^{\circ} 24' 49''$ N, $24^{\circ} 46' 28''$ E). The metasandstone is exposed in association with black shales and black metachert of the Bali formation. It contains rounded quartz clasts and lithic clasts, including mica schists and black metachert, within a matrix of fine-grained white mica, greenish biotite, quartz, albite and opaque phases (Fig. 2f). Micas are enriched at boundaries to clasts perpendicular to the foliation, forming strain caps around the elongate clasts (Fig. 2f). The long axis of the clasts is aligned parallel to the foliation of the metaconglomerate defined by a general shape preferred orientation (SPO) of all components (Fig. 2e, f). The clasts are comprised of coarse-grained quartz, fine-grained-sericite quartzites, elongated clasts of micaschists, black shales and black chert, as well as coarse-grained albite–quartz clasts. Metamorphic albite porphyroblasts occur with their internal foliation oriented oblique to the external

foliation. The vein quartz clasts show large quartz grains with marked undulose extinction and subgrains and a high amount of fluid inclusions, often aligned as trails.

The sample contains 100–260 μm sized detrital zircons (Fig. 5a) with a large amount of Precambrian U–Pb ages (Figs 6, Fig. 7a, b, 8a). Most abundant are the Neoproterozoic detrital zircons (60%; Fig. 7a; Table S1, in the Supplementary Material available online at <https://doi.org/10.1017/S0016756819001365>). This age group is dominated by Ediacaran zircons (36%) with age peaks at 562 ± 6 Ma and 611 ± 4 Ma, followed by 18% Cryogenian detrital zircons (Figs 7b, 8a). Only three zircons are Tonian in age (between 900 and 1000 Ma). There is also a significant number of Palaeozoic zircons (27%) consisting of Early Carboniferous zircons (11%, age peak at 343 ± 7 Ma; Figs 7a, 8a), Early Ordovician zircons (5%, age peak at 484 ± 6 Ma; Figs 7a, 8a) and Late Cambrian zircons (9%, age peak at 502 ± 5 Ma; Figs 7a, 8a). Only a small number of zircons (12%) are between 1 Ga and 2.8 Ga old. The presence of Early Carboniferous zircons is consistent with a Late Carboniferous / Early Permian age of the host rocks. One zircon shows a younger age (271 ± 6 Ma); however, it is only 90% concordant and the $^{207}\text{Pb}/^{206}\text{Pb}$ age is at 302 ± 37 Ma. The youngest concordant zircon is dated at 334 ± 7 Ma (Fig. 7a). The larger part of the zircons in all age groups is rounded or anhedral (Fig. 6). Of the Palaeozoic zircons c. 40% are euhedral, in the Neoproterozoic age group only ~20% are euhedral and the zircons older than 1 Ga are generally well rounded (Fig. 6). Some of the zircons show pitted surfaces (Fig. 5a, zircon A85; 334 ± 7 Ma).

4.b. Lower Fodele formation (LS154)

The Fodele formation in its lower part consists of metasandstones and black shales interlayered with dark dolomite marbles. In the upper part, mainly dark dolomite marble occurs, which is typically rich in fossil relics (e.g. Epting *et al.* 1972; König & Kuss, 1980). For U–Pb analysis a metasandstone (LS154; $35^{\circ} 23' 41''$ N, $24^{\circ} 55' 27''$ E) was sampled in the central Talea Ori at Pera Galinos, which is the largest outcrop of the lower Fodele formation, located within the non-inverted (normal) limb of the large-scale fold structure of the Talea Ori group (Fig. 1; Richter & Kopp, 1983; Seybold *et al.* 2019). The metasandstone is foliated at an angle to the bedding and forms several dm-thick layers interlayered with phyllitic rocks (Fig. 9a). It comprises angular quartz grains that are 200 to 400 μm in diameter and surrounded by a phyllosilicate-rich matrix (Fig. 9b). A minor amount (c. 1%) of angular albite clasts of a few hundred μm in diameter occurs (Fig. 9b). On microscopic scale, bedding and foliation are hardly recognizable (Fig. 9b).

The metasandstone of the lower Fodele formation contains 80–200 μm sized detrital zircons with mainly Precambrian ages (80%; Figs 6a, 7c; Table S2, in the Supplementary Material available online at <https://doi.org/10.1017/S0016756819001365>). The dominant Neoproterozoic age group (57%) is split into three equal parts (Fig. 7d; 20% Ediacaran, 17% Cryogenian, 20% Tonian zircons). There are 9% zircons with Stenian age. The age peak at 611 ± 4 Ma is similar to the Ediacaran age peak of the Bali formation (Fig. 8). In contrast to the Bali formation, there are also age peaks at 678 ± 6 Ma ($n=5$) in the Cryogenian, and at 878 ± 10 Ma ($n=3$) and 977 ± 11 Ma ($n=6$) in the Tonian (Fig. 8). Palaeoproterozoic and Archaean zircons are less abundant (13%) and are mostly rounded (~90%; Figs 5b, 6a). For the Palaeozoic zircons (20%) the highest age peak is at the Silurian/Devonian boundary, dated at 414 ± 4 Ma ($n=4$). The analysis of the two youngest zircons defines a U–Pb age at 326 ± 5 Ma

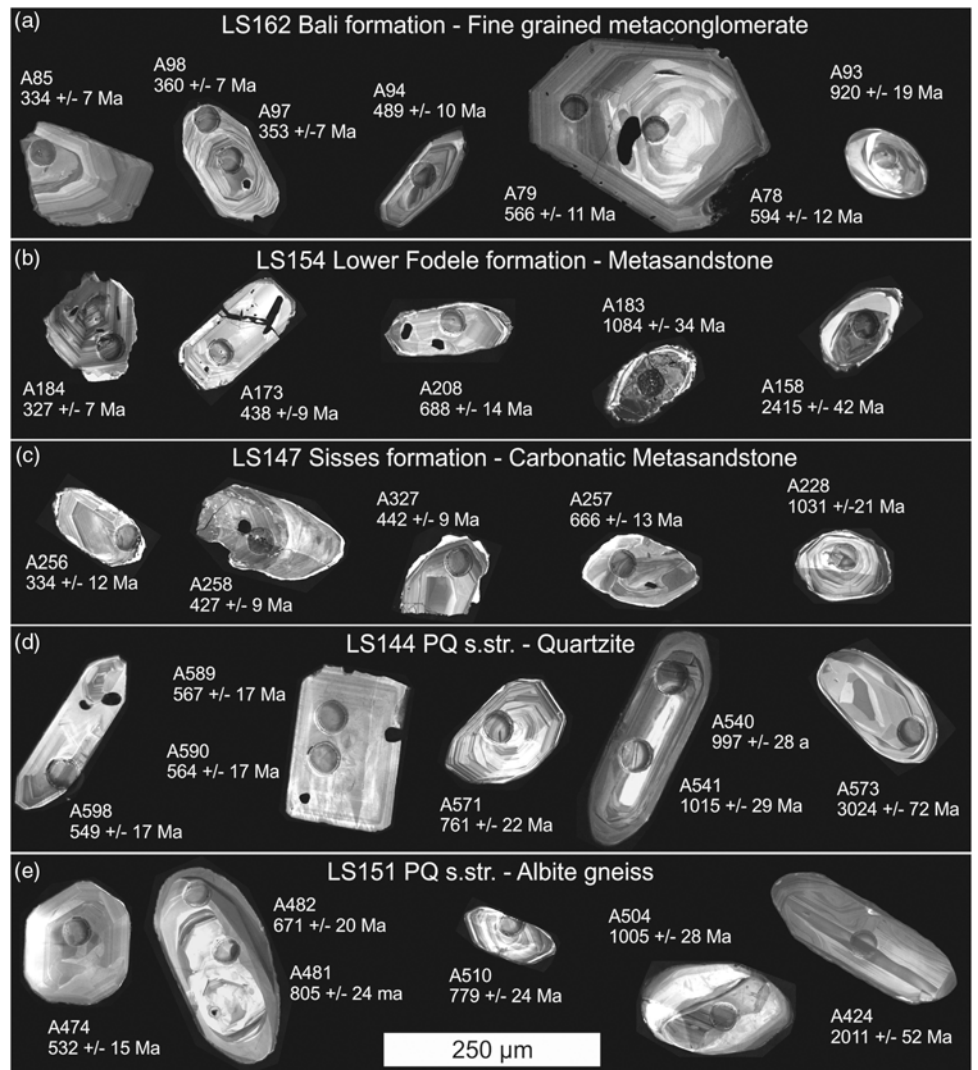


Fig. 5. Representative cathodoluminescence (CL) images of analysed zircons. Apparent $^{206}\text{Pb}/^{238}\text{U}$ ages are reported with 2σ uncertainty.

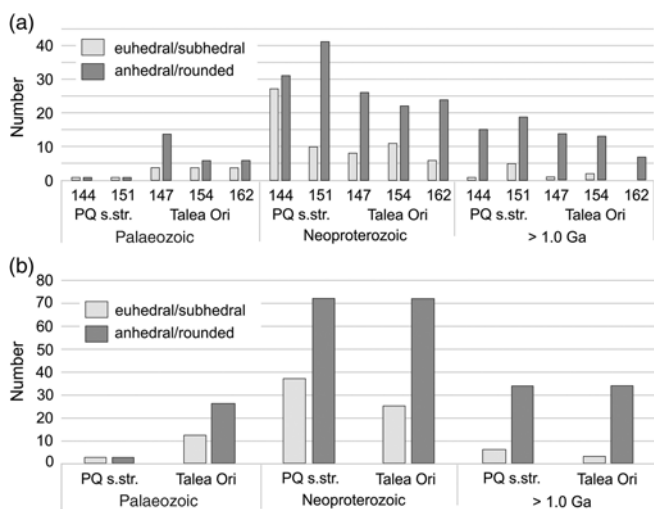


Fig. 6. Number of euhedral and subhedral vs anhedral and rounded zircons within (a) each of the five different samples LS 144, LS151, LS162, LS147, LS154 and (b) the PQ s.str. (LS144 + LS151) and the Talea Ori group (LS162, LS147, LS154).

(Carboniferous), which is compatible with the Middle Permian biostratigraphic age of the Fodele formation (Pseudofusulina and Parafusulina zones (Epting *et al.* 1972), corresponding to Artinskian to Kungurian (Kozur & Krahl, 1987; Zhang & Wang, 2018)). The zircons of the lower Fodele formation sample often show pitted surfaces, but in general the proportions of rounded/ angular to euhedral or subhedral zircons are similar to the proportions within the Bali formation sample, of c. 60 % anhedral/ rounded zircons within the Palaeozoic group and >70 % in the Neoproterozoic age group (Fig. 6a).

4.c. Sisses formation (LS147)

The Sisses formation comprises marbles and violet to greenish phyllites interlayered with metasandstones and carbonatic metaconglomerates (Fig. 9c–f). Epidote (Fig. 9f) and albite blasts occur with a high amount of inclusions forming internal fabrics usually oblique to the external foliation of the rock, which is typical for porphyroblast formation in the Talea Ori, as described e.g. for albite (Theye, 1988; Zulauf *et al.* 2016; Seybold *et al.* 2019) and chloritoid (Chatzaras *et al.* 2006). The carbonatic

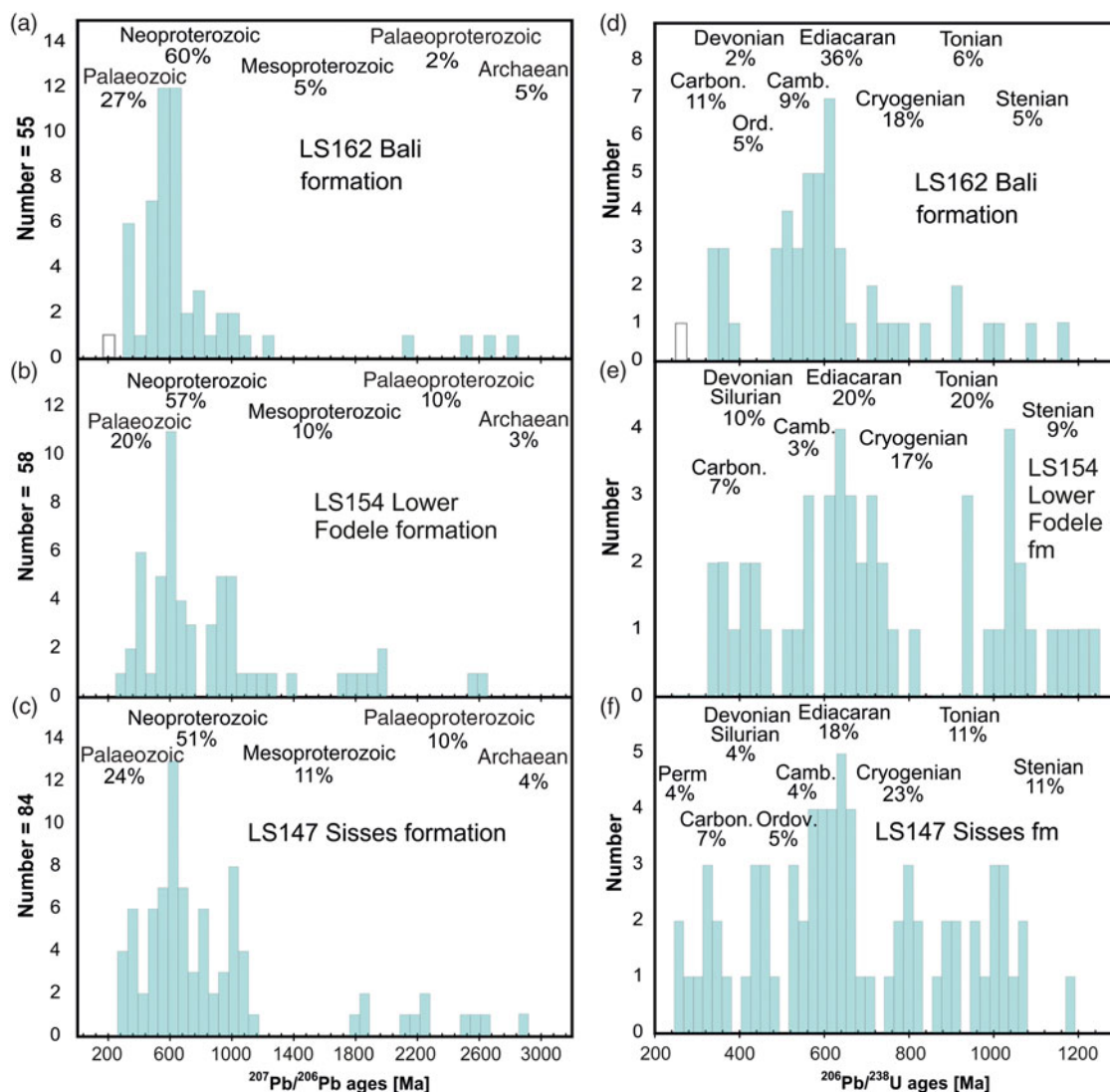


Fig. 7. Density plots of detrital zircons separated from the Bali formation (LS162), lower Fodele formation (LS154) and Sisses formation (LS147) of the Talea Ori group. Complete ranges are plotted against the $^{207}\text{Pb}/^{206}\text{Pb}$ age, and for younger zircons the $^{206}\text{Pb}/^{238}\text{U}$ age is shown. Bin width = 40, concordance 90% to 110%.

metaconglomerates comprise carbonatic clasts up to ~5 cm in diameter with strain caps and strain shadows (Fig. 9e, f). The strain shadows form as complex pressure fringes composed by elongate calcite and quartz grains \pm mica (Fig. 9f). The carbonatic clasts contain various relic shapes of recrystallized fossil material, which was investigated in a metaconglomerate by Kock *et al.* (2007). For U–Pb analysis, a sample from a carbonatic metasandstone was collected close to the contact to the Fodele formation (LS147; Fig. 1; 35° 23' 34" N, 24° 53' 51" E). The metasandstone is foliated oblique to the bedding, which is apparent from darker layers enriched in opaque phases (Fig. 9c, d). It consists mainly of quartz and calcite and a small amount of albite, with grain diameters of 200–500 μm (Fig. 9d).

The sample LS147 contains, like the samples from the Bali and Fodele formations, a high amount of Precambrian detrital zircons (76%). Half of the detrital zircons (51%) show Neoproterozoic ages with 17% Ediacaran, 23% Cryogenian and 11% Tonian detrital zircons (Fig. 7e, f). The Ediacaran age peaks are similar to the samples described above at 563 ± 7 Ma ($n=6$) and 605 ± 7 Ma ($n=7$). The other Neoproterozoic age peaks are different in the Cryogenian at 647 ± 8 Ma ($n=7$) and at 808 ± 7 Ma

($n=5$). The Stenian-aged zircons (11%) are the only Mesoproterozoic input (Fig. 7e, f). Together with the Tonian zircons they define an age peak at the Neoproterozoic/Mesoproterozoic boundary at 1027 ± 19 Ma ($n=5$; Fig. 8c) which is typical for zircon ages of the Grenvillian orogeny. A smaller amount (14%) of the zircons is older than 1.6 Ga (Fig. 7e). The Palaeozoic detrital zircons (24%) display similar age peaks such as in the Fodele and Bali formations in the Ordovician at 455 ± 10 Ma ($n=5$) and in the Early Carboniferous at 330 ± 4 Ma ($n=4$). Early Permian detrital zircons occur with the youngest age peak at 269 ± 3 Ma ($n=3$, Fig. 8), which is compatible with the Olenekian deposition age of the Sisses formation (König & Kuss, 1980). An analysis of an angular zircon yields a $^{206}\text{Pb}/^{238}\text{U}$ age of 118 ± 2 Ma (concordance of 96%; Table S3 in the Supplementary Material online at <https://doi.org/10.1017/S0016756819001365>), which is too young compared to the deposition age. This analysis could be influenced by low-temperature Ca-rich fluids, which caused a strong lead loss. Seven discordant zircons with U–Pb ages from *c.* 70 to 190 Ma also point to a later lead loss. The Sisses formation sample contains the smallest number of euhedral zircons of all three samples of the Talea Ori group.

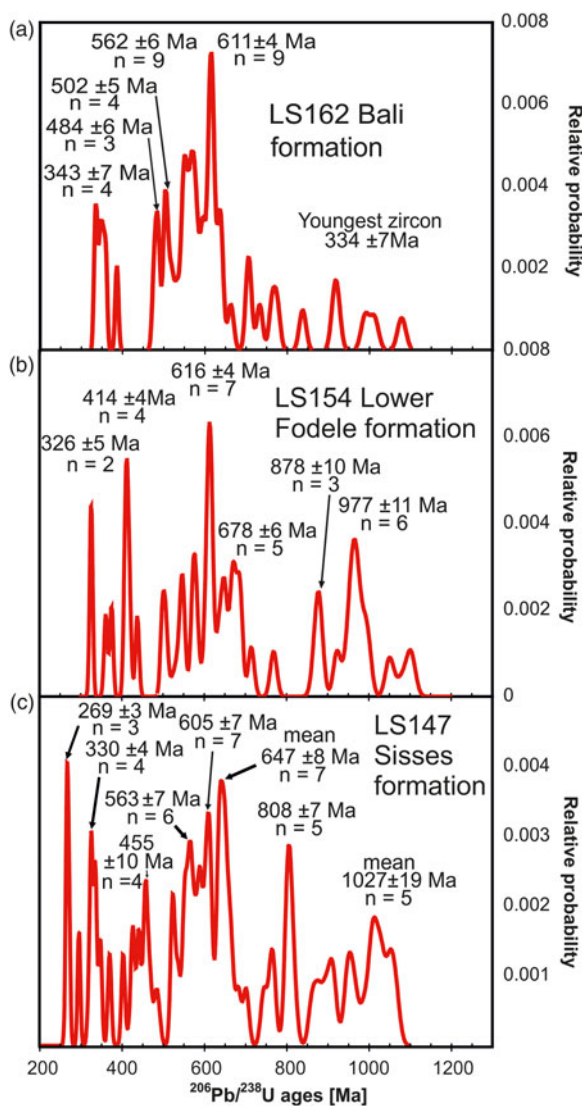


Fig. 8. Probability curves with age peaks of Bali formation, lower Fodele formation and Sisses formation of the Talea Ori group.

Especially in the Palaeozoic age group, there is a larger number of anhedral/rounded zircons (Fig. 6a) than in LS154 (Fodele formation) and LS162 (Bali formation).

4.d. Phyllite-Quartzite unit s.str.

From the PQ s.str., a quartzite from the central Talea Ori (LS144) and an albite gneiss from the eastern Talea Ori (LS151) were collected (Fig. 1).

4.d.1. Quartzite (LS144)

The quartzite (LS144; Fig. 1; 35° 24' 24" N, 24° 52' 17" E) interlayered with phyllites crops out a few metres south and structurally below a marble at the hill of Skilarmi, SE of the village of Almyrida. Conodonts in the marble indicate the biostratigraphic age to be Olenekian (Epting *et al.* 1972; König & Kuss, 1980). It has been discussed whether this marble at Skilarmi belongs to the Olenekian Sisses formation rather than being part of the PQ s.str. In the discussion, Kuss & Thorbecke (1974) proposed that the marble was tectonically emplaced within the phyllites and quartzites, whereas Richter & Köpp (1983) suggested that the

metasediments south of the marble also belong to the Sisses formation. According to our observations, the marble layers are strongly deformed (just like the phyllites and quartzites next to it) but they represent sedimentary layers: marble layers, with cm thickness to 0.5 m thickness, and calcitic phyllites are interlayered with the phyllites and quartzites.

The quartzite is composed of elongate quartz grains of variable diameter (100 µm to 1 mm) forming a weak foliation by their SPO (Fig. 10a, b). The boundaries of quartz grains are coated with fine-grained iron oxides and mica (<1%), and small amounts of tourmaline (<1%) occur. Euhedral zircon grains up to ~80 µm size are visible in thin-section (Fig. 10b). The quartz grains show undulatory extinction and locally deformation lamellae (Fig. 10b); however, it is not clear if these features are inherited from a deformed host rock or if this is due to Alpine deformation.

The sample contains mainly Precambrian zircons (99%; Table S4, in the Supplementary Material online at <https://doi.org/10.1017/S0016756819001365>). The main U–Pb age group of the detrital zircons is the Neoproterozoic group (80%), which is dominated by the Ediacaran zircons (37%; Fig. 11a–c), with age peaks at 571 ± 9 Ma ($n = 9$), 599 ± 4 Ma ($n = 13$), 624 ± 5 Ma ($n = 8$), and by the subhedral to euhedral Cryogenian zircons (32%) with smaller age peaks at 661 ± 6 Ma ($n = 6$) and at 794 ± 8 Ma ($n = 6$). Only 11% Tonian zircons occur, with a tiny peak at 972 ± 8 Ma ($n = 4$). Stenian (5%) zircons are the only Mesoproterozoic zircons (Fig. 11c). There are 14% zircons with U–Pb ages larger than 1.6 Ga, which are mostly rounded (Fig. 6a). Two concordant analyses of one Ordovician zircon yield a U–Pb age at 466 ± 10 Ma (Fig. S4, in the Supplementary Material available online at <https://doi.org/10.1017/S0016756819001365>), which is the youngest zircon. The quartzite contains the highest number of euhedral zircons of all the samples analysed in this study, most of which occur in the Neoproterozoic age group (~45%; Fig. 6a).

4.d.2. Albite gneiss (LS151)

Sample LS151 is an albite gneiss, collected NE of Fodele (Fig. 1; 35° 23' 41" N, 24° 56' 23" E). The albite gneiss is interlayered with dark greenish albite schists, characteristic of the PQ s.str. It is composed of several mm-thick layers comprising lens-shaped larger quartz and albite grains (typically 500–700 µm in diameter; Fig. 1c) within a fine-grained (typically ~50 µm in diameter; Fig. 10d) matrix of quartz, albite, iron oxides and micas. Layers rich in larger clasts occur interlayered with mm-thick layers devoid of larger clasts, comprised purely of fine-grained elongate quartz and mica (Fig. 1c, d). Subhedral isometric zircons of up to ~140 µm size are visible in thin-section (Fig. 10d). The larger grains show strain caps and strain shadows, with their long axis and the alignment of the micas forming a pronounced foliation. A second cleavage (shear band cleavage, cf. Seybold *et al.* 2019) with enrichment of micas along the shear band boundaries is present (Fig. 1c).

The sample contains two zircons of Early Cambrian age and otherwise only Precambrian zircons (Fig. 11d–f). The prominent U–Pb age group of the detrital zircons is the Neoproterozoic group (70%), which is dominated by Cryogenian zircons (35%), and the highest age peak is in the Ediacaran (Fig. 11d) at the boundary to the Cryogenian at 625 ± 5 Ma ($n = 11$). The age peaks at 673 ± 6 Ma ($n = 5$) and at 807 ± 11 Ma ($n = 8$) are similar to the Cryogenian age peaks of sample LS144 and there is an additional age peak at 727 ± 7 Ma ($n = 9$). The Ediacaran zircons (15%) are less abundant, with a prominent age peak close to the Cambrian boundary at 544 ± 6 Ma ($n = 6$), which is the youngest concordant zircon population of the sample. In the Tonian age group (20%)

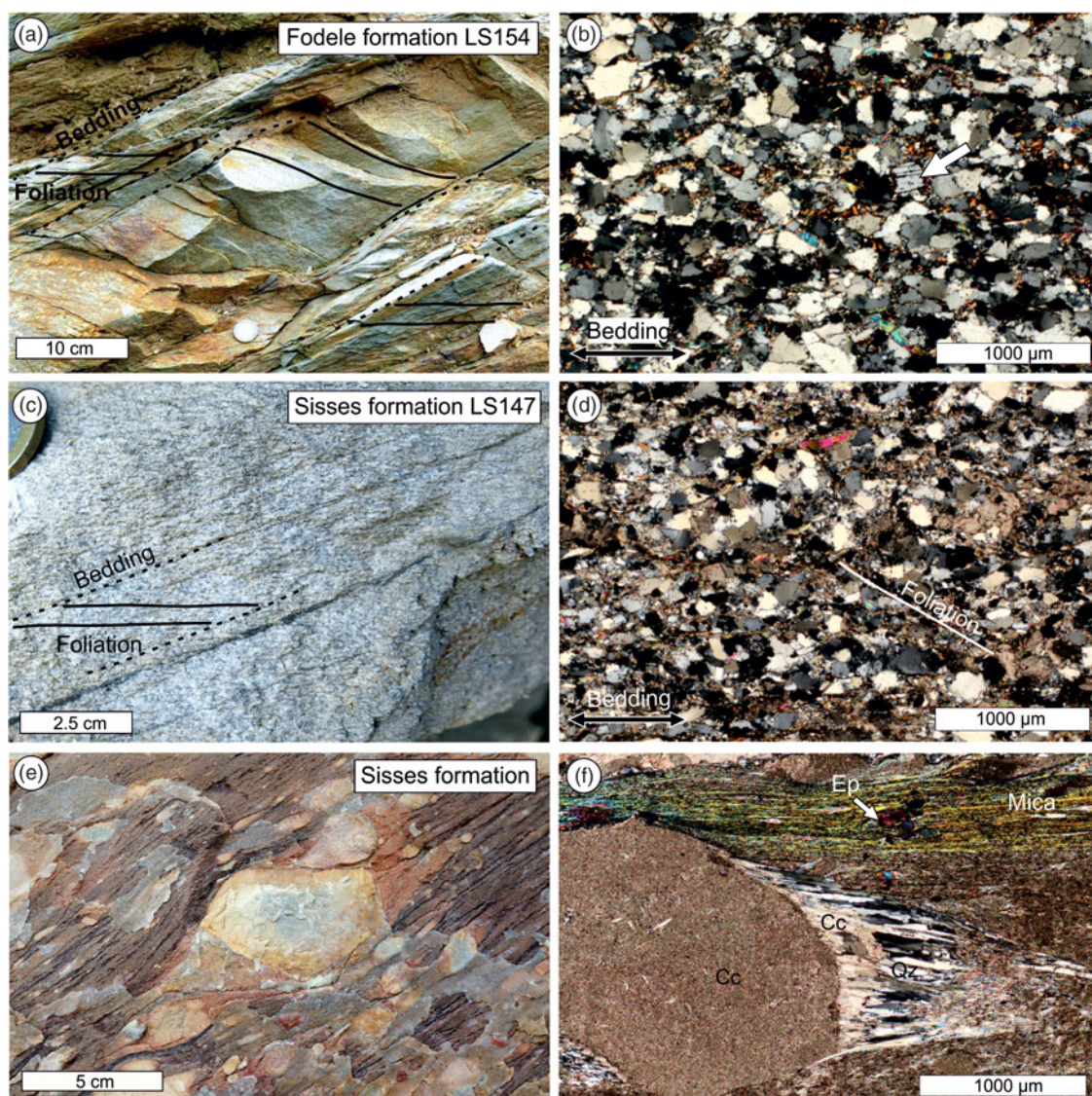


Fig. 9. Lower Fodele formation and Sisses formation of the Talea Ori group. (a, b) Metasandstone of the lower Fodele formation at Pera Galinos; the sample in (b) was collected for U–Pb dating of detrital zircons. It is composed mainly of quartz and smaller amounts of mica, iron oxides and albite (arrow). (c, d) Carbonatic metasandstone of the Sisses formation, collected for U–Pb dating of detrital zircons; the foliation forms an angle to the bedding. (e, f) Carbonatic metaconglomerate of the Sisses formation (New Road east of Sisses). Carbonate clasts form complex strain shadows composed of calcite (Cc), quartz (Qz) and mica. In the mica-rich layers of the matrix epidote, blasts with a high amount of inclusions occur.

there is an age peak at 913 ± 11 Ma ($n = 5$). The Stenian zircons (13%), together with the early Tonian zircons, define a prominent age peak at the Neoproterozoic/Mesoproterozoic boundary (Fig. 11d) at 1011 ± 8 Ma ($n = 11$), which is typical of zircon ages of the Grenvillian orogeny. The Palaeoproterozoic zircons occur with 14%, which is the highest percentage of all samples. They define an age peak at 2011 ± 11 Ma ($n = 4$). Archaean zircons (2%) are scarce (Fig. 11f). The zircons are mostly anhedral or rounded and a small number of zircons are euhedral to subhedral (Fig. 6a).

5. Discussion

Our data show characteristically different zircon age spectra of the metasediments in the Talea Ori of central Crete. Including the detrital zircon age spectra obtained by Zulauf *et al.* (2016) and Kock *et al.* (2007), three different zircon age spectra are

distinguished (Figs 12, 13). (1) The Carboniferous to Triassic quartzites of the PQ s.str. are dominated by Precambrian zircons (LS151 and LS144; Figs 12, 13). (2) The metasandstones of the Upper Carboniferous / Lower Permian Bali formation, sampled south of the port of Bali (Kock *et al.* 2007; Zulauf *et al.* 2016), have a prominent U–Pb zircon age peak in the Late Carboniferous with scarce older Palaeozoic (<3%) input (Bali A; Fig. 12). (3) The Lower Permian coarse-grained metasandstone of the Bali formation, sampled west of Bali village, the metasandstones of the Middle Permian lower Fodele formation and the Olenekian Sisses formation all show similar age spectra, with Early Palaeozoic and Early Carboniferous age peaks and a high number of Neoproterozoic zircons (LS162, LS154, LS147; Fig. 12).

In the following, we discuss the provenance of the siliciclastic metasediments in the PQ s.str. and in the Talea Ori group. All available data will be balanced with respect to the provenance of the siliciclastic metasediments. The different detrital zircon

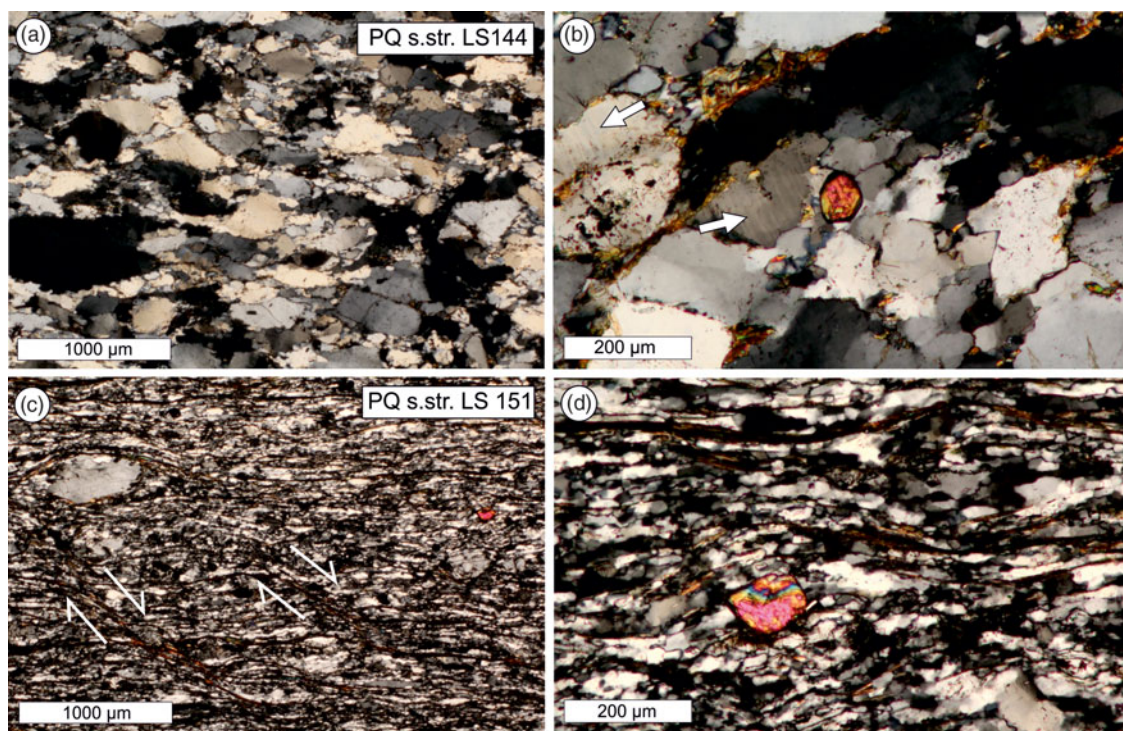


Fig. 10. Photomicrographs of samples from the PQ s.str. collected for U-Pb dating of detrital zircons (crossed polarizers). (a, b) Quartzite LS144 (Skilarmi) shows irregular-shaped elongate quartz grains with sutured grain boundaries. Close-up (b) shows deformation lamellae in quartz grain, left to euhedral zircon. (c, d) Albite-gneiss NW of Fodele shows layers with fine-grained quartz and larger albite clasts as well as subhedral to euhedral zircon grains (d).

U-Pb age spectra and our lithological analyses lead to four alternative models for the palaeogeographic and tectonic configurations of the nappes of the External Hellenides.

5.a. Stratigraphic age and sedimentary source regions of the PQ s.str

5.a.1. Stratigraphic age of the PQ s.str. in central Crete

The youngest concordant zircon population defines a Late Ordovician maximum sedimentation age. The only fossil record for a biostratigraphic age, conodonts from a marble at Skilarmi, points to an Olenekian deposition age in central Crete (Epting *et al.* 1972). It was, however, suggested that this marble is associated with the Sisses formation, which is Olenekian in age (Kuss & Thorbecke, 1974; König & Kuss, 1980; Richter & Kopp, 1983). Here, we can refute this suggestion since the age spectrum obtained by U-Pb dating of detrital zircons in the quartzite (LS144; Figs 12, 13), which is located a few metres structurally below and south of the Skilarmi marble, is characteristic of the PQ s.str. (Chatzaras *et al.* 2016; this study) and differs clearly from that of the Talea Ori group. This implies that the rocks exposed south of the Skilarmi marble are part of the PQ s.str. and the Olenekian age of the marble (Epting *et al.* 1972) can be taken as the valid biostratigraphic age of the PQ s.str. in central Crete. This age is consistent with Carboniferous to Triassic biostratigraphic ages known for the PQ s.str. in western and eastern Crete (Krahl *et al.* 1983, 1986; Zulauf *et al.* 2018).

5.a.2. U-Pb ages and source regions of the PQ s.str. detrital zircons

The samples from the phyllites and quartzites in the Talea Ori are dominated by 96 % (Cr114, Zulauf *et al.* 2016) to 99 % (LS151,

LS144 this study) Precambrian zircons with a small amount of Cambrian (533 ± 6 Ma, $n = 4$) to Ordovician (479 ± 10 Ma, $n = 5$) zircons (Fig. S5, in the Supplementary Material online at <https://doi.org/10.1017/S0016756819001365>). There are similar high numbers of zircons with Ediacaran and Cryogenian ages (Fig. 11). The amount of Tonian-aged zircons varies from 11 to 26 % and is sometimes higher than the amount of Ediacaran zircons (LS151, Fig. 11). There are pronounced Early Ediacaran age peaks around 600 Ma, and high Tonian/Stenian age peaks at c. 1000 Ma, the latter pointing to a strong input of zircons formed at the Grenvillian orogeny (Fig. 12). Typical of the zircon age spectrum is a Mesoproterozoic age gap between 1.12 and 1.6 Ga (Fig. 12a) and the high amount of Cryogenian zircons. This excludes the Amazonian craton (West Gondwana) and related Avalonian-type terranes, like the Pelagonian zone, as the source area for the studied metasediments, because these do not show an age gap in the Mesoproterozoic (Fig. 13).

Instead, the Sahara Metacraton (SMC; Fig. 13) is suggested as one of the possible sources of the detrital zircons analysed from the PQ s.str. in central Crete. The SMC is built up of Neoproterozoic to Palaeoproterozoic domains, which were overprinted in Neoproterozoic time (e.g. Meert & Van Der Voo, 1997; Abdelsalam *et al.* 2002; Johnson & Woldehaimanot, 2003; and references therein). The Neoproterozoic detrital zircons of the present study (Fig. 11) correlate with the orogenic events associated with the assembly of the SMC, the Arabian-Nubian Shield and East Gondwana (e.g. Stern, 1994; Abdelsalam *et al.* 2002; Kröner & Stern, 2005; Küster *et al.* 2008; Morag *et al.* 2011a, b). In the West African Craton some of the Neoproterozoic events and the age gap from 1.1 Ga to 1.6 Ga as described above are also known. However, there are no latest Mesoproterozoic (Stenian) / Early Neoproterozoic (Tonian) events, which are yet significant for

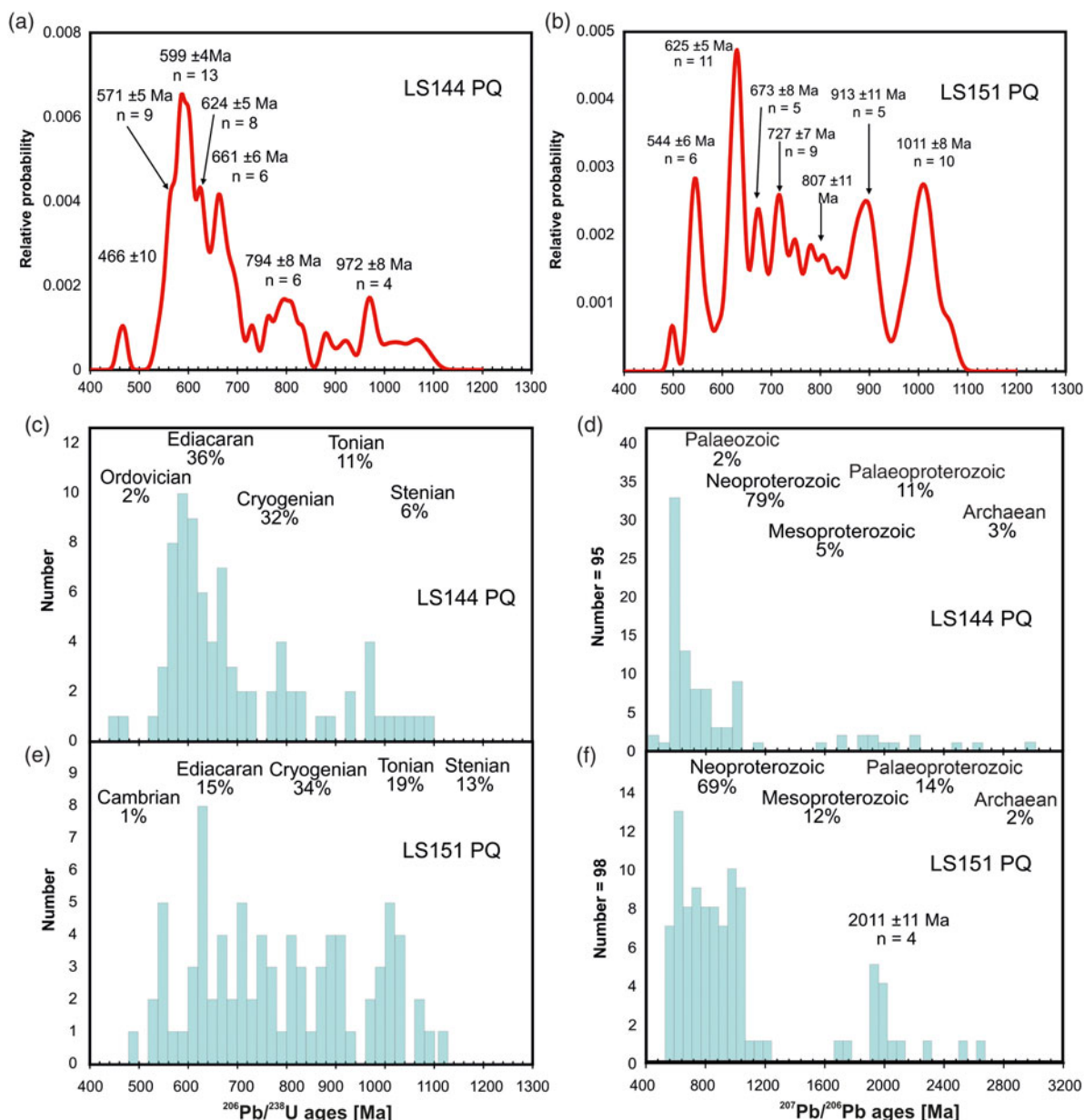


Fig. 11. Probability curves (a, d) and density plots (b, c, e, f) of detrital zircons from quartzite (LS144) and albite-gneiss (LS151) of the PQ s.str.

the zircon spectra of the sediments from the PQ s.str. Tonian and Stenian zircons are known from the eastern margin of the SMC at the contact to the Arabian–Nubian Shield in northern Sudan (Küster *et al.* 2008), from xenocrysts in Pan-African granites of the Western Desert of Egypt (Bea *et al.* 2010) and from the Sa'al metamorphic complex in South Sinai (Be'eri-Shlevin *et al.* 2009b, 2012). These ages correspond well with the Tonian/Stenian age peak at *c.* 1000 Ma of the PQ s.str. of central Crete. The rounded Neoproterozoic (50%) and Tonian/Stenian (90%) zircons in the metasediments of the PQ s.str. can also be explained by the recycling of Cambrian to Devonian sediments from Libya (Meinhold *et al.* 2011), Egypt and the Middle East (Israel and Jordan; Be'eri-Shlevin *et al.* 2009b). The Cambrian detrital zircons and the latest Ediacaran age peak of euhedral zircons at 547 ± 5 Ma (*n* = 9) from the three PQ s.str. samples of central Crete (Zulauf *et al.* 2016; this study) point to the Cadomian arc as possible source area, which occurs along the north Gondwana margin (granitoids

in the Mendere Massif; Zlatkin *et al.* 2013). The Cadomian magmatic arc was partly detached from the northern margin of Gondwana and survived inside the East Gondwana derived terranes (Minoan terranes (Zulauf *et al.* 2007); NE Sicily (Williams *et al.* 2012); Peloponnesus (Dörr *et al.* 2015); Crete (Romano *et al.* 2004)). East Africa and the Middle East are unlikely source regions for the numerous 540–555 Ma old zircons because igneous activity younger than 570 Ma was extremely rare in this region (Be'eri-Shlevin *et al.* 2009a; Morag *et al.* 2011a, b; Avigad *et al.* 2012). Thus, the latest Ediacaran and Cambrian zircons most probably stem from the remaining Cadomian arc. A possible source region of the metasediments of the PQ s.str., thus, is the former northern margin of East Gondwana with the SMC and the Arabian–Nubian Shield together with their Palaeozoic cover sediments.

In comparison to detrital zircon age spectra of sandstones from northern Africa (e.g. Avigad *et al.* 2003; Kolodner *et al.* 2006;

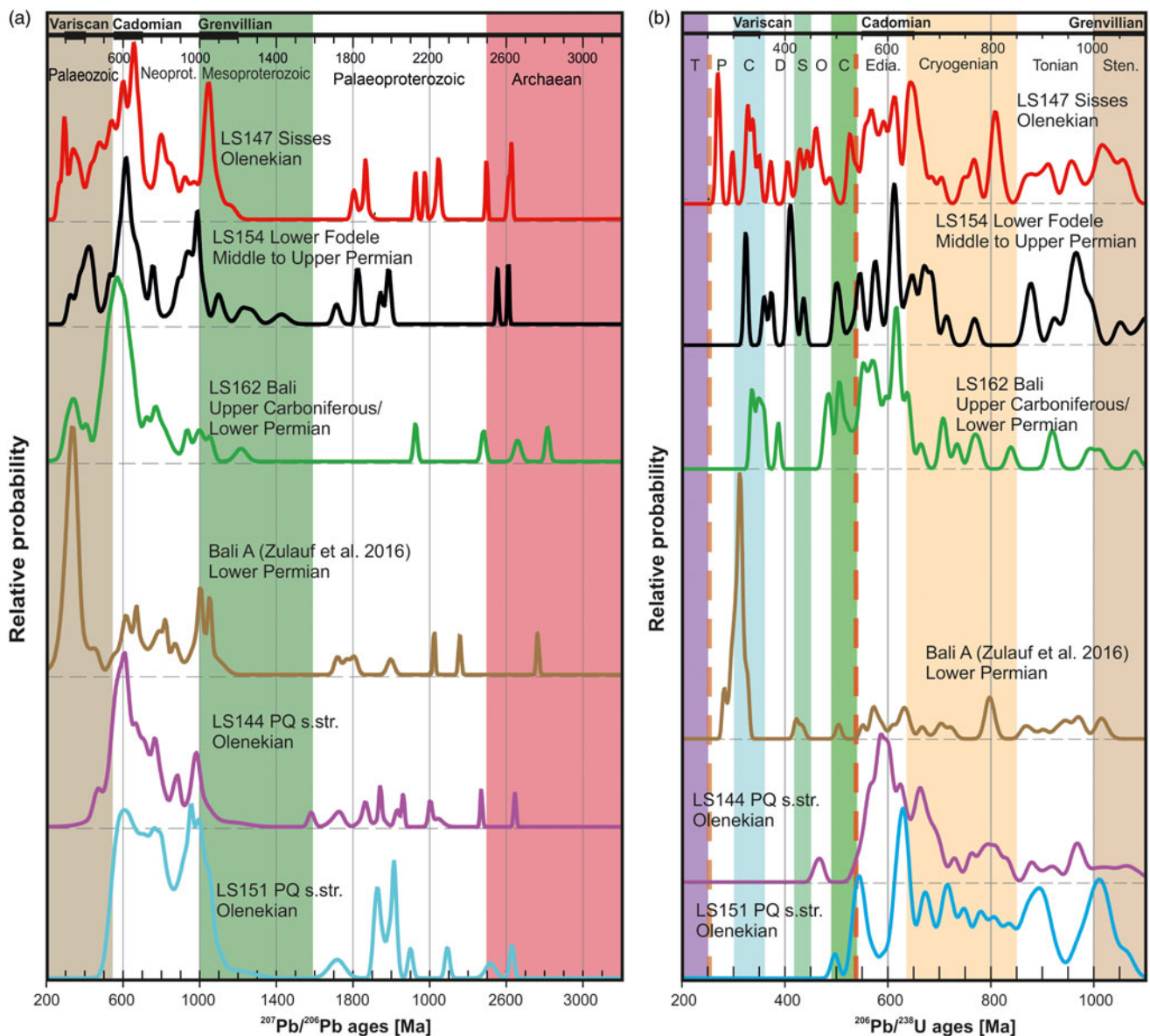


Fig. 12. Comparison of the probability curves of the samples of the Talea Ori group and the PQ s.str. (a) data from 200–3200 Ma, (b) data from 200–1200 Ma.

Linnemann *et al.* 2011; Meinhold *et al.* 2011; Avigad *et al.* 2012), the detrital zircon age spectra of the quartzites of the PQ s.str. from central Crete correlate well with the age spectra of the Carboniferous and Triassic sandstones of Libya (Meinhold *et al.* 2011). These Libyan sandstones also contain the same young zircons from the Ordovician (3%) and Cambrian (7%) together with 540 Ma age peaks (Meinhold *et al.* 2011). The Neoproterozoic age group displays the same composition as the quartzites of the PQ s.str. with 22% Ediacaran, 23% Cryogenian and 11% Tonian zircons. The Stenian detrital zircons have a 17% presence. There is also an age gap between 1.1 Ga and 1.6 Ga, typical for East Gondwana, with only 17% zircons older than 1.6 Ga. Because of this similarity of the detrital zircon age spectra of the unmetamorphosed Libyan cover sediments and the PQ s.str., both should have shared the same source area at the northern margin of Gondwana until the PQ s.str. was detached from Gondwana during Triassic times (e.g. Zulauf *et al.* 2018).

In summary, the age spectra of detrital zircons of the Olenekian quartzites of the PQ s.str. of central Crete correlate well with

known age spectra of the PQ s.str. (Fig. 14) from other occurrences on Crete (Chatzaras *et al.* 2016; Zulauf *et al.* 2016, 2018), Kythira and Peloponnesus (Marsellos *et al.* 2012; Kydonakis *et al.* 2014; Chatzaras *et al.* 2016) and Samos (Löwen *et al.* 2015). The inferred palaeogeographic position of the PQ s.str. is at the northern margin of East Gondwana (Fig. 15; Zulauf *et al.* 2015, 2016, 2018; Chatzaras *et al.* 2016). This is consistent with what is expected based on sedimentological, structural and regional arguments (e.g. Kozur & Krahl, 1987; Dornsiepen & Manutsoglu, 1994; Dornsiepen *et al.* 2001; Stampfli *et al.* 2003; Robertson, 2006).

5.b. Zircon age spectra and sedimentary source regions of the Talea Ori group

The detrital zircon age patterns of three metasandstones sampled south of Bali port close to the contact to the PQ s.str., analysed by Zulauf *et al.* (2016) and Kock *et al.* (2007), show a distinctly different pattern compared to the PQ s.str. (representative sample Bali A by Zulauf *et al.* 2016 is shown in Figs 12, 13). The highest age peak

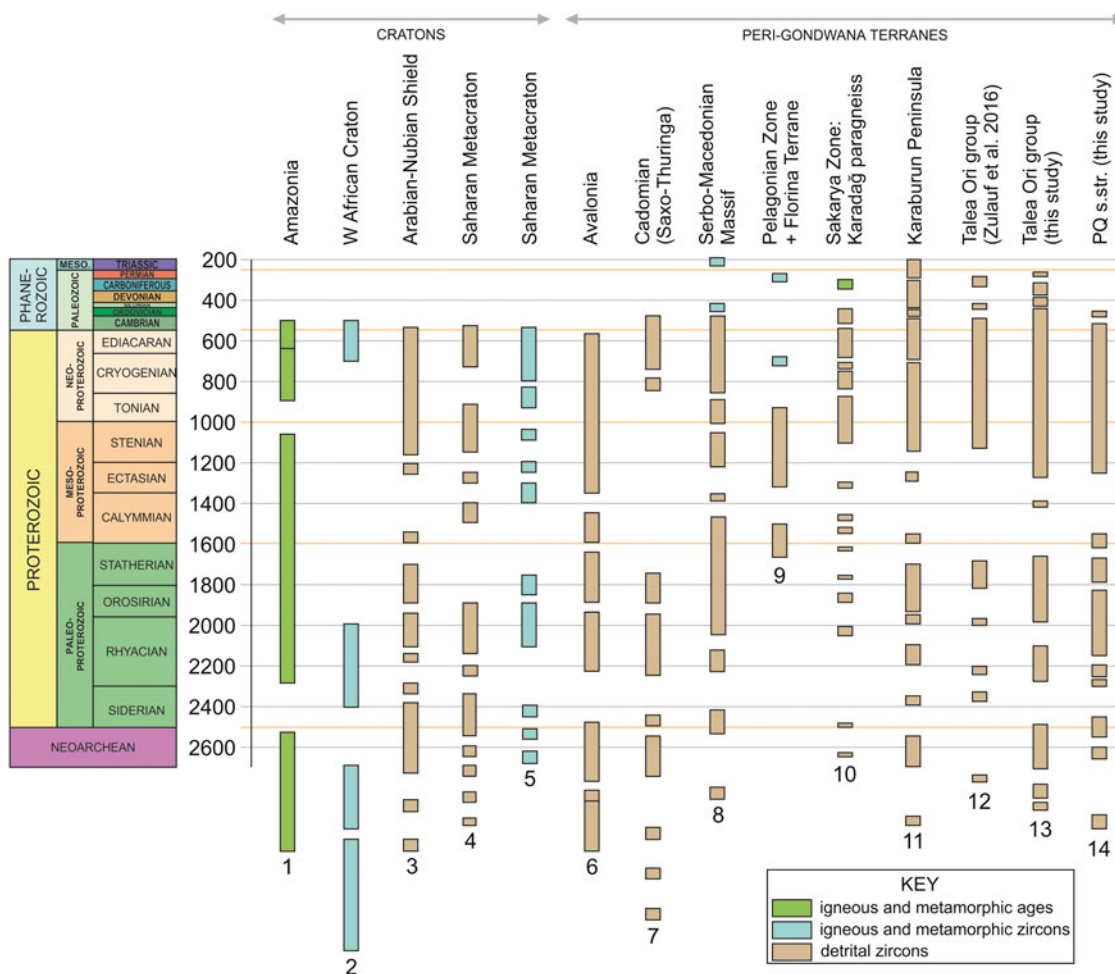


Fig. 13. Distribution of detrital/igneous/metamorphic zircon ages and igneous/metamorphic events known from major cratons and peri-Gondwana terranes, modified after Ustaömer *et al.* (2013), in comparison to data from the Talea Ori (12–14). Data sources: 1, Friedl *et al.* (2004), Nance *et al.* (2008); 2, Friedl *et al.* (2004), Linnemann *et al.* (2004), Murphy *et al.* (2004 a,b); 3, Drost *et al.* (2011) and references therein; 4, Drost *et al.* (2011) and references therein, Meinhold *et al.* (2011); 5–7, Drost *et al.* (2011) and references therein; 8, Himmerkus *et al.* (2007, 2009), Meinhold *et al.* (2010), Pirgadiikia and Vertiskos Terranes belonging to the Serbo-Macedonian Massif; 9, Himmerkus *et al.* (2007) and references therein; 10, Ustaömer *et al.* (2013); 11, Löwen *et al.* (2017); 12, Zulauf *et al.* (2016); 13–14, this study.

is in the Late Carboniferous, and older Palaeozoic zircon ages are scarce (<3 %), whereas in the PQ s.str. there are no zircon ages <450 Ma. Concerning the number of Precambrian zircons, the three samples are heterogeneous: the samples from Zulauf *et al.* (2016) contained 55 % (Bali A, Fig. 12a) and 17 % (Bali B) of Precambrian zircons. The sample from Kock *et al.* (2007), with 23 analysed zircons, contains a similar amount of 26 % Precambrian zircons. The Proterozoic age spectrum resembles the age spectrum of the PQ s.str., with the Neoproterozoic zircons having similar high amounts of Ediacaran and Cryogenian ages, an age peak at around 1 Ga and a Mesoproterozoic age gap (Fig. 12a). Such zircon spectra were suggested to be characteristic of the ‘Minoan terranes’, as introduced by Zulauf *et al.* (2007), who derived them from East Gondwana. According to Zulauf *et al.* (2015), prior to the Carboniferous these Minoan terranes collided with Eurasia along the Eurasian margin. In general, the Minoan terrane-type zircon spectra are zircon spectra that can be correlated with East Gondwana, i.e., NE Africa – Arabia, which nowadays are known from Iberia, the Pyrenees, the Alps, the Serbo-Macedonian Massif and Turkey (Dörr *et al.* 2015; Stephan *et al.* 2019). The Late Carboniferous / Early Permian zircons (33 to 65 %) in the meta-sandstones are commonly euhedral (Kock *et al.* 2007; Zulauf

et al. 2016), suggesting a proximal source. According to Zulauf *et al.* (2016), the metasandstones south of Bali port are derived from the Late Variscan orogen situated at the southern active margin of Eurasia (see discussion in Zulauf *et al.* 2016, 2018, and references therein).

The detrital zircon age spectra of the samples from the Bali formation west of Bali (LS162), the Fodele formation (LS154) and the Sisses formation (LS147), analysed in this study (Figs 12, 13), are similar to each other but strikingly different to the detrital zircon age spectra of the samples south of the port of Bali (Kock *et al.* 2007; Zulauf *et al.* 2016), as well as different to those from the PQ s.str. (Fig. 12). Compared to the metasandstones from south of Bali port, the change of the highest age peak from the Late Carboniferous to the Ediacaran is one of the main differences (Fig. 12a). The amount of Late Carboniferous zircons drops from a maximum of 66 % (Kock *et al.* 2007; Zulauf *et al.* 2016) to 0–1 % in the samples of the Bali, Fodele and Sisses formations. The Palaeozoic age record is dominated by Early Palaeozoic rather than Late Palaeozoic input (Fig. 13). Only a small proportion of the Palaeozoic zircons are euhedral, similar to the proportion within the Neoproterozoic group (Fig. 6b). In general, the samples of the Talea Ori group show an even higher proportion

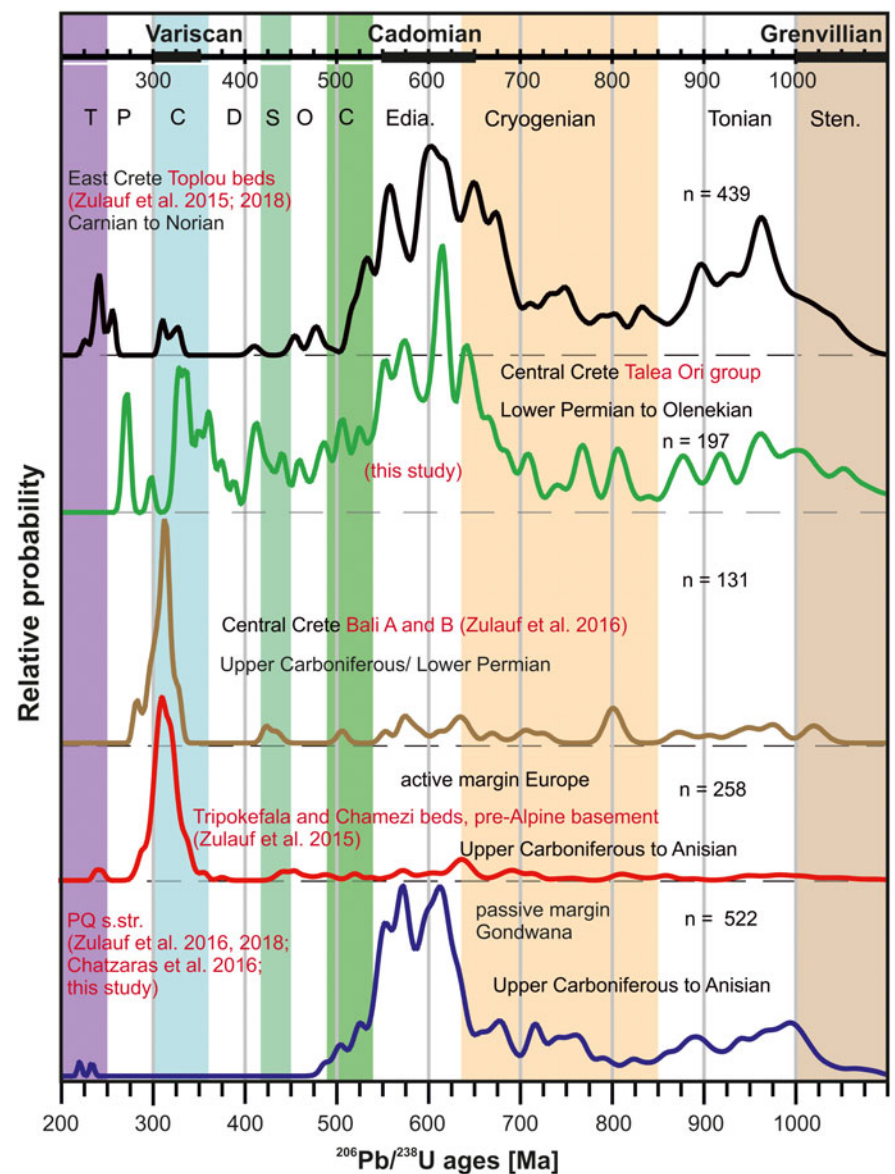


Fig. 14. Comparison of probability curves from different units exposed on Crete.

of anhedral/rounded zircons vs euhedral zircons than the samples of the PQ s.str. (Fig. 6b), and a large part of them are rounded to angular, partly with pitted surfaces (especially in the Fodele formation, sample LS154; Fig. 5b). This is in contrast to the Late Carboniferous zircons of the Bali formation from south of Bali port, that are dominated by euhedral zircons (Kock *et al.* 2007; Zulauf *et al.* 2016). The Neoproterozoic age group varied in the metasandstones south of Bali port between 5% and 45%, whereas in the new samples it is constant around 55%. The Proterozoic zircons show, as in all other samples from the Talea Ori, a NE Africa – Arabia-type age spectrum, with the Neoproterozoic zircons having similar amounts of zircons with Ediacaran and Cryogenian ages with age peaks at around 0.6 Ga and 1 Ga (Figs 8, 12) and a considerable amount of Tonian/Stenian zircons (Fig. 12a).

Despite the differences in age spectra, the samples south of the port and the sample of the Bali formation analysed in this study belong to the same sedimentary sequence, as evidenced by their interlayering with the characteristic black metachert and black schists (Kock *et al.* 2007; Seybold *et al.* 2019). All analysed samples

from the Bali formation are located close to the contact to the PQ s.str. (Fig. 1; Kock *et al.* 2007; Zulauf *et al.* 2016). The samples of the Bali formation west of Bali (this study) are probably of slightly higher stratigraphic position compared to the samples from the thick black metasandstones south of the port analysed in the former studies. This is indicated on the one hand by their respective structural positions within the overturned fold limb, but due to the strong tectonic overprint within the shear zone (Seybold *et al.* 2019) it is ambiguous to derive a relative age from the structural position between two samples. The heterogeneity of the different zircon spectra within the Bali formation at the base of the Talea Ori group is suggested to be due to sediment delivery from different source areas. This assumption is supported by the high lithological diversity of components within the siliciclastic rocks of the Bali formation (e.g. Figs 2–4).

5.b.1. Origin of lithoclasts, Bali formation

The component analysis of the quartz metaconglomerate of the Bali formation indicates that the pebbles are derived from several different source areas. The black metachert (c. 4% of the

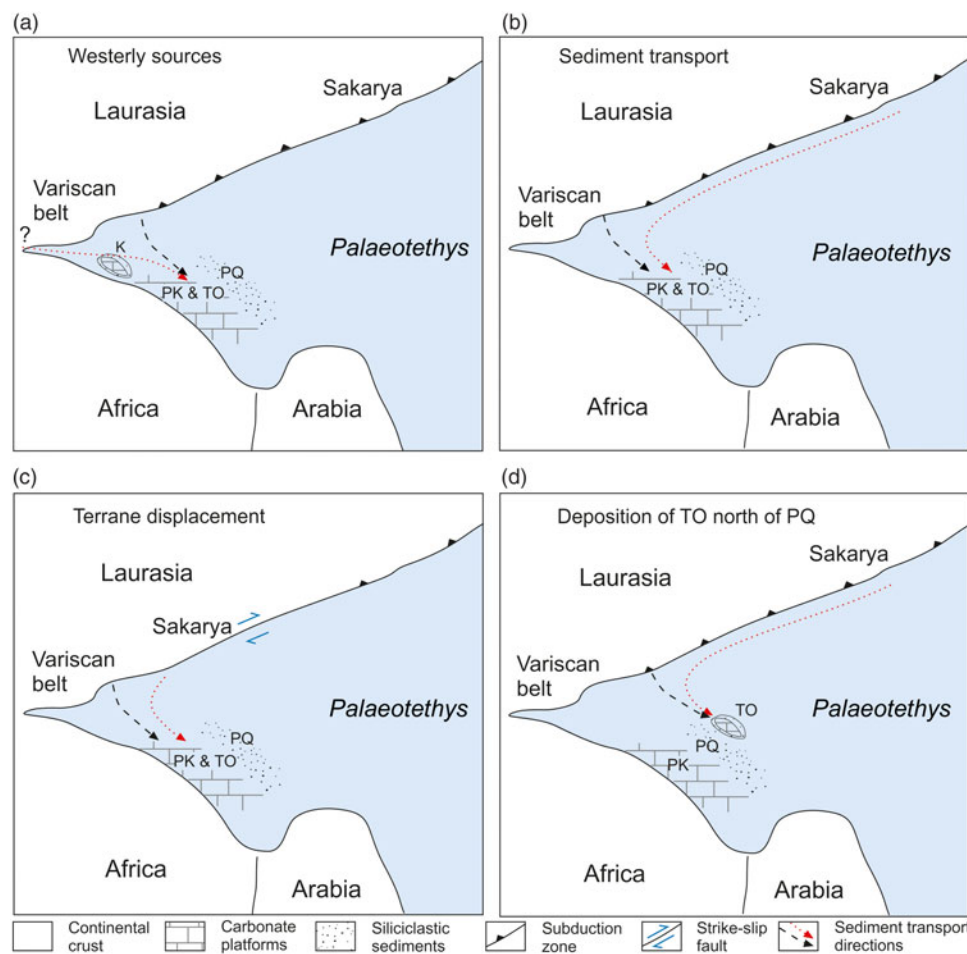


Fig. 15. Alternatives for the palaeogeographic configurations of the lower tectonic nappes of the Cretan nappe pile from Late Carboniferous / Early Permian to Olenekian times. Dashed arrows indicate directions of sediment transport (black dashed arrows = transport of euhedral Variscan-aged zircons; red dotted arrows = transport of rounded zircons with Silurian, Devonian and Early Carboniferous U–Pb ages). (a) Distal sediment transport from westerly yet unspecified sources, modified after Ustaömer *et al.* (2019). (b) Distal sediment transport from the Sakarya Zone. (c) Eastward terrane displacement of the Sakarya Zone after deposition of the lower Talea Ori group. Blue/grey arrows indicate dextral displacement that should have happened after Olenekian times. (d) Deposition of the Talea Ori group north of the PQ s.str. Abbreviations are: Sakarya Zone (Sk), Phyllite-Quartzite unit s.str. (PQ), Plattenkalk unit (PK), Talea Ori (TO), Karaburun sediments (K).

pebbles) as well as metapelitic and metapsammitic clasts (*c.* 6 % of the pebbles) are most probably derived from a local source, as the Bali formation is in large part made up of metasandstones, shales and metachert. The elongate shapes and similarity of the black metachert clasts to the stratiform chert layers within the Bali formation, as well as the low resistance to weathering and transport of the metapelitic and metapsammitic clasts, are consistent with a proximal and presumably intraformational source. These types of pebbles make up less than 10 % in the conglomerate (Fig. 4). In contrast, the pebbles derived from felsic volcanic rocks, mica schists and black vein quartz have a very good rounding (Fig. 2a), indicating a rather distal source, consistent with the observation that such rocks are not exposed anywhere in the Talea Ori. Despite the indicated distal source, these pebbles form more than 80 % of the components. This large amount of ‘exotic’ components reveals a complex source of detritus. The proportions of the different types of pebbles vary greatly in different outcrops of the conglomerate, from pure meta-quartz conglomerates to pure intraformational metaconglomerates/breccias, indicating an active environment in a slope setting with ongoing change in deposition conditions in Late Carboniferous to Early Permian times. The metaconglomerates and metasandstones indicate a strong terrigenous influx while the contemporaneous black metachert with radiolarians points to pelagic conditions. The rare patch reefs (cropping out exclusively at Bali beach), in contrast, point to a shallow marine environment. The sequence is consistent with a tectonically

unstable setting in which sediments were deposited by turbiditic currents.

5.b.2. Zircon age spectra and lithological comparison to eastern Crete

The metasandstones of the Bali formation south of Bali port (Fig. 14, yellow colour; Zulauf *et al.* 2016) and the upper Rogdia beds from the eastern Talea Ori show a similar detrital zircon age pattern to a coeval Lower Permian black quartzite of pre-Alpine basement from eastern Crete, interpreted as active margin signature of Europe (Fig. 14, red colour; Zulauf *et al.* 2015). Zulauf *et al.* (2016) therefore suggested that in the Late Carboniferous / Early Permian a similar Late Variscan basement fed the Bali formation in central Crete and the pre-Alpine basement observed in eastern Crete.

The overlying Upper Carboniferous / Lower Permian to Olenekian formations of the lower Talea Ori group, analysed in our study, show a similar zircon age spectrum (Fig. 14, green probability curve) to that of the upper formation of the Tyros units, the Toplou beds (Fig. 14, black probability curve; Zulauf *et al.* 2015): a high amount of Neoproterozoic zircons together with Grenvillian input points in both cases to East Gondwana-derived terranes as source areas. However, the Upper Triassic Toplou beds of eastern Crete cannot be correlated with the lower Talea Ori group because the Toplou beds display only a few Ordovician to Devonian zircons with no age peaks, and their stratigraphic age is much younger than the age of the metasediments of the lower Talea Ori group. The U–Pb age spectrum of detrital zircons from the Talea Ori group

in general contains more Early Palaeozoic zircons than the other spectra from Crete. Therefore, despite some similarities in the zircon spectra of the Talea Ori group and the Tyros unit, there are significant differences in the zircon spectra, indicating different source areas.

Both units are different in tectonic position, with the Talea Ori group structurally below and the Tyros unit structurally above the PQ s.str. They have different stratigraphic ages as well as metamorphic grade (amphibolite facies metamorphism of pre-Alpine basement quartzite). Furthermore, the lithologies of the siliciclastic/carbonatic sequence of the Talea Ori group and the metavolcanic Tyros unit are very different.

The differences in zircon spectra, lithologies and structural position suggest that the deposition area of the Talea Ori group was different from that of the Tyros unit. The source region for the Lower Permian metasandstones south of Bali port and pre-Alpine basement quartzite of eastern Crete was similar (Late Variscan basement), but from the Early Permian to the Olenekian the source region of the Talea Ori group cannot be correlated with the source region of the Tyros unit.

5.b.3. Source regions of detrital zircons in the lower Talea Ori group

The Ordovician U–Pb age peaks of the detrital zircons of the lower Talea Ori group at 455 ± 10 Ma ($n = 4$) and 484 ± 6 Ma ($n = 3$) can be correlated with Ordovician granitoids of the basements dated with U–Pb analyses on zircons from the West Sakarya zone (Biga Peninsula; 462 ± 6 Ma, Özmen & Reischmann 1999), from Armutlu Peninsula (Boundary to the Istanbul zone; 470 Ma, Okay *et al.* 2008a), from the Tavşanlı Zone correlated with the Taurides (446 ± 8 Ma, Özbey *et al.* 2013; 467 ± 5 Ma, Okay *et al.* 2008b) and from the Serbo-Macedonian Massif (460 ± 8 Ma, Titorenkova *et al.* 2003; 452 ± 17 Ma, Meinhold *et al.* 2010). The Silurian age peak of the Bali, Fodele and Sisses formations at 435 ± 5 Ma ($n = 4$, mean age) can be correlated to the Silurian basement with orthogneisses of the Serbo-Macedonian Massif (U–Pb analyses on zircons at 425 Ma to 443 Ma; Himmerkus *et al.* 2006, 2009). The Early Devonian age peak at 414 ± 4 Ma ($n = 4$) of the U–Pb analyses of detrital zircons of the Talea Ori group (central Crete) is similar to the Devonian ages in NW Turkey of metagranodiorite from the Biga peninsula (390 to 400 Ma; Okay *et al.* 1996, 2006). Aysal *et al.* (2012a) and Sunal (2012) dated five granitoids of the West Sakarya Zone (NW Turkey) with U–Pb zircon ages from 390 to 401 Ma. Their wall rocks are metasediments which contain a U–Pb age spectrum of detrital zircons with a dominant Ediacaran age peak and two age peaks during the Tonian and one at 1 Ga. Aysal *et al.* (2012b) interpreted the amount of 6% Mesoproterozoic zircons of the age spectrum of the detrital zircons of the wall rock as Avalonian/Amazonian related, but if we consider the Tonian- and Stenian-aged zircons as one age group (11%, Grenvillian) then only 3% zircons with an age between 1.15 Ga and 1.6 Ga are left. Tonian and Stenian zircons are common in the Central and East Sakarya Zone and are similar to the U–Pb age spectra of detrital zircons of NE Africa – Arabia (Stephan *et al.* 2019) and East Gondwana derived terranes (Zulauf *et al.* 2007). Late Devonian granitic–granodioritic gneisses, dated at around 370 Ma from the northern (Sea of Marmara) and southern (Aegean Sea) part of the Biga peninsula (Özmen & Reischmann, 1999; Pb/Pb single-zircon), are slightly older than the U–Pb age peak at 362 ± 4 Ma ($n = 4$, mean age) of the Late Devonian detrital zircons of the Talea Ori group. Ustaömer

et al. (2012) dated a granitoid with a similar U–Pb age at the Devonian/Carboniferous boundary (358 ± 5 Ma) of the Eastern Sakarya Zone which intruded into the Karadağ paragneiss.

Late Carboniferous to Early Permian (325 to 280 Ma) granitoids are abundant in the Eastern Mediterranean region and have been reported from the Hellenides, the Cycladic islands and the Sakarya Zone (see compilation in Meinhold *et al.* 2008; Löwen *et al.* 2017) whereas plutons of Early Carboniferous age (325 to 355 Ma) are not known from the Eastern Mediterranean region. The oldest Carboniferous plutons have zircon ages around 325 Ma described from orthogneisses of the central Cyclades (Engel & Reischmann, 1998, 1999), of the External Hellenides (Kithira Island, Xypolias *et al.* 2006) and the Central and East Sakarya Zone (Ustaömer *et al.* 2012, 2013). The only U–Pb ages of zircons from the basement of the Eastern Mediterranean region, which correlate with U–Pb ages of the Early Carboniferous detrital zircons of the Talea Ori group, are metamorphic rims with ages of 344 ± 4 Ma and 337 ± 4 Ma grown around Late Devonian and Ediacaran zircons from the Karadağ paragneiss of the Eastern Sakarya Zone (Ustaömer *et al.* 2013).

The Karadağ paragneiss from the Variscan high-grade overprinted basement also reveals a detrital zircon age spectrum (Ustaömer *et al.* 2013) similar to that of the Talea Ori group. Not taking into account the *c.* 335 Ma old metamorphic zircons, the U–Pb age spectrum of the detrital zircons of the Karadağ paragneiss again displays Precambrian zircons with zircon ages of NE Africa – Arabia affinity (Grenvillian zircons up to 32%) with dominant Ediacaran/Cryogenian input (46%). The rounded Palaeozoic zircons are similar to those of the Talea Ori group, with only 27% abundance. Mainly Cambrian and Ordovician zircons (18%), together with the few Devonian zircons (8%), point to a distal position to the Devonian source rocks.

Early Palaeozoic to Early Carboniferous ages (500 Ma to 340 Ma), as mentioned above, of the Eastern Mediterranean region are typical for the internal zones of the Variscan belt from central Europe. Late Cadomian, Cambrian and rift-related Ordovician granitoids are described from the Saxothuringian Zone (Vesser Complex and the Polish West Sudetes; Kröner *et al.* 2001; Linnemann *et al.* 2007, 2008 and references therein), the Moldanubian Zone (Teplá-Barrandian Unit and Mariánské Lázně Complex; Teufel, 1988; Bowes and Aftalion 1991; Dörr *et al.* 1998; Timmermann *et al.* 2006), the French Massif Central, the Armorican Massif and the Allochthonous Complex in Spain (Da Silva *et al.* 2016 and references therein). Early Variscan Silurian and Devonian ages are known from granodiorite gneisses of the northern Saxothuringian Zone (Böllstein Odenwald and Spessart; Lippolt, 1986; Dombrowski *et al.* 1995; Brätz, 2000; Zeh *et al.* 2000, 2003; Reischmann *et al.* 2001) from the Saxothuringian/Moldanubian boundary (Teufel, 1988) and from Moldanubian basement (Teplá-Barrandian Unit and Mariánské Lázně Complex; Timmermann *et al.* 2004, 2006). The Devonian thermal event from 370 to 390 Ma is widespread in crystalline basement of the Central European Variscides. Devonian monazite and zircon U–Pb ages are known from the allochthonous units of the Saxothuringian Zone (Münchberger nappe pile metamorphic grown zircons at 390 ± 3 Ma; Koglin *et al.* 2018), from the Moldanubian Zone (Teplá-Barrandian Unit and the Mariánské Lázně Complex; 380 to 387 ± 3 Ma, isotope dilution thermal ionization mass spectrometry (ID-TIMS) (Timmermann *et al.* 2004, 2006)) and from the Central Armorican Domain (Armorican Massif, Schulz, 2013).

Early Variscan granitic rocks are also known from the Slavonian mountains (NE Croatia), Tisia unit (Tisza unit), with cooling ages between 423.7 ± 12.9 and 321.5 ± 8 Ma (Pamić & Jurković, 2002). There, also metamorphic rocks of Ordovician to Silurian age are exposed with monazite ages of 444 ± 19 Ma and 421 ± 10 Ma (Pamić & Jurković, 2002; Balen *et al.* 2006). However, age data and outcrops of the concerned rocks seem to be rare, and also the palaeogeographic position during Permian time seems not to be well constrained so far (Pamić & Jurković, 2002). Moreover, the dated pre-Variscan metamorphism was low-grade (350–400 °C); therefore, a delivery of Palaeozoic pre-Variscan aged zircons from this region is ambiguous.

The Sakarya Zone and Serbo-Macedonian Massif of the Eastern Mediterranean and Slavonian mountains of NE Croatia are equivalent to the internal zones of the Variscides of central Europe, whereas the Cycladic islands and parts of the Hellenides are suggested to represent a Late Carboniferous to Early Permian active margin at the southern margin of Eurasia (Zulauf *et al.* 2015, 2016, 2018). Based on the comparison of the zircon data, in the Talea Ori group one of the source areas during the Early Permian might be the southern active margin of Eurasia, which fed the metasandstones at the base of the Bali formation with euhedral Late Carboniferous zircons (50 to 80 %, 300 to 315 Ma). The second source area during the Early Permian until Olenekian (Bali, Fodele, Sisses formations) could be represented by the Sakarya Zone with East Gondwana-derived basement and Early Palaeozoic granitoids, which formed the hinterland of the active margin.

Similar zircon age spectra to those in the lower Talea Ori group have also been detected in the Karaburun Peninsula and Chios island. The Upper Carboniferous to Permian Küçükbağçe formation of the Karaburun Peninsula also contains pre-Cambrian zircons with a NE Africa–Arabia-type age spectrum, but more Palaeozoic zircons (35–45 %) than the Talea Ori group. There are mainly Early Carboniferous zircons (10–16 %) and Devonian zircons (8–12 %). The Cambrian zircons have a similar amount (7–12 %) to that of the Talea Ori group (9 %). The Lower Triassic sample of the Gerence formation contains 55 % Devonian detrital zircons (Löwen *et al.* 2017). These authors therefore suggested that the Sakarya Zone represents the Devonian basement acting as proximal source for the Karaburun sediments, because of the similarities of the zircon spectra. However, recent analyses show that the $\varepsilon_{\text{Hf}(t)}$ values of the Devonian zircon populations differ significantly from the $\varepsilon_{\text{Hf}(t)}$ values of the Devonian granites in the Sakarya Zone (Ustaömer *et al.* 2019). Accordingly, Ustaömer *et al.* (2019) suggested westerly sources such as granitic rocks of the Aegean or central Europe, rather than the Sakarya Zone, for the Karaburun sediments, which are suggested to restore to the northern margin of Gondwana.

In summary, the zircon age spectra and the lithological characteristics of the lower Talea Ori group indicate that different sedimentary source areas have to be assumed. One source area delivered Late Carboniferous euhedral zircons (300 to 320 Ma; Kock *et al.* 2007; Zulauf *et al.* 2016), which point to a late Variscan basement as source area, similar to the pre-Alpine basement of the Tyros unit from East Crete (Zulauf *et al.* 2015). This late Variscan basement was proximal to the deposition of the Bali formation in Late Carboniferous/Early Permian times. From the Late Carboniferous / Early Permian onwards to the Olenekian, however, sediment transport to the Talea Ori group was dominated by zircons with Cambrian to Early Carboniferous ages

and Neoproterozoic ages indicating East Gondwana derivation (NE Africa – Arabia affinity). The good rounding of these zircons points to a distal source region. The comparison of the zircon age spectra of the Talea Ori group to currently existing zircon data reveals that the Sakarya Zone and southern active margin of Eurasia have to be discussed as probable source regions. Also, a yet unspecified westerly source in the Aegean region or central Europe needs to be considered, as suggested by Ustaömer *et al.* (2019), as source for the Karaburun sediments, which reveal similar zircon age spectra. Based on lithological and structural observations, we will further discuss the source areas and the implications for the palaeogeographic positions.

5.c. Implications for the palaeogeographic position of the Talea Ori group and association with the Plattenkalk unit

In the following, we discuss four alternative scenarios to reconcile the sedimentological and structural arguments with the zircon data of the Talea Ori group (Fig. 15). The first alternative considers sediment transport from westerly sources other than the Sakarya Zone, consistent with a palaeogeographic position of the Talea Ori group at the northern margin of Gondwana in the western Palaeotethys, as it is also assumed for the Plattenkalk unit with which the Talea Ori group is generally associated (e.g. Soujon *et al.* 1998; Dornsiepen *et al.* 2001; Stampfli *et al.* 2003; Robertson, 2006, 2012; Kock *et al.* 2007). If the Sakarya Zone, however, represents the main distal source region for the Talea Ori group, the sediment transport to the Talea Ori group needs to be discussed, as in most Late Carboniferous to Early Triassic palaeogeographic reconstructions of the Eastern Mediterranean the Sakarya Zone restores to the southern margin of Eurasia to the east of the Pelagonian Zone and Rhodope (e.g. Stampfli *et al.* 2003; Okay *et al.* 2006). Therefore, the second and third alternatives discuss a sediment current from the Sakarya Zone at the southern margin of Eurasia and terrane displacement of the Sakarya Zone to the east. The fourth alternative is that the Talea Ori group was deposited to the north of the PQ s.str. and therefore might not be associated with the Plattenkalk unit.

5.c.1. Sediment transport from westerly sources

Consistent with sedimentological studies (Robertson & Pickett, 2000; Okay *et al.* 2006; Robertson & Ustaömer, 2009), Ustaömer *et al.* (2019) suggested a westerly sediment source for the Karaburun sediments, which have similar zircon age spectra to the Talea Ori group. Sediment transport from westerly sources to the Talea Ori group at the northern margin of Gondwana has been suggested already by Kock *et al.* (2007); however, the suggested sources – Spain, Calabria, Algeria or Morocco – almost exclusively provide zircons of Late Carboniferous / Early Permian age, except for central Iberia where a small number of Early Carboniferous zircon ages were reported (Montero *et al.* 2004). The rounded zircons of Devonian and Silurian age in the Talea Ori group, therefore, cannot be explained by transport from Spain, Calabria, Algeria or Morocco, but should be derived from more internal zones of the Variscan orogeny. Ustaömer *et al.* (2019) suggested still unidentified sources in the west, such as the Aegean or central Europe, to explain the Devonian zircons in the Karaburun sediments. In this alternative, sediments were eroded in the west, transported eastwards and deposited by turbidity currents up to several hundreds of kilometres to the east (Ustaömer *et al.* 2019). Such a setting may also be possible for the Talea Ori metasediments (Fig. 15a). However, the euhedral

Variscan-aged zircons in the metasediments of the Bali formation rather point to a proximal source and are not consistent with such a long-distance sediment transport. Furthermore, the unknown westerly sediment sources are not yet specified by zircon age spectra and, as the similarity of the zircon age pattern of the Talea Ori group to the Sakarya zone is quite striking, the Sakarya Zone as source region and its palaeogeographic implications will be explored in the following three alternatives.

5.c.2. Sediment transport from sources at the southern margin of Eurasia

Sources at the southern margin of Eurasia were considered possible by Kock *et al.* (2007) under the condition of southward subduction of the Palaeotethys Ocean (Şengör *et al.* 1984). Even if during Permian and Triassic times rather northward subduction is assumed (e.g. Stampfli & Borel, 2002), southward subduction (or double subduction) has been inferred at least during Carboniferous times for some regions in the South Aegean (e.g. Romano *et al.*, 2006; Xypolias *et al.* 2006; Zulauf *et al.* 2008) and Turkey (e.g. Göncüoğlu *et al.* 2007; Robertson & Ustaömer, 2009; Candan *et al.* 2016). Transport from northerly sources to the Talea Ori group was also considered possible under the condition that the PQ s.str. is interpreted as a post-Variscan rift basin that filled near sea level by Late Triassic times (Robertson, 2012). Assuming a palaeogeographic model in which the Palaeotethys was closed by Late Carboniferous times (e.g. Robertson, 2006; Ustaömer *et al.* 2019) and deep troughs existed in the N–S direction (e.g. Crasquin-Soleau *et al.* 2006), sediment transport from a northerly origin may be plausible (Fig. 15b). However, a main problem with sediment transport from north to south is that the PQ s.str., which restores to the north of the Talea Ori group (e.g. Dornsiepen *et al.* 2001), systematically lacks Middle to Late Palaeozoic ages and Variscan zircons (Chatzaras *et al.* 2016; Zulauf *et al.* 2016, 2018). Therefore, currents bringing sediment from the north should have transported sediment exclusively to the Talea Ori group and not to the PQ s.str., to which, in contrast, sediment was only delivered from Gondwana in the south.

5.c.3. Terrane displacement

In a tectonically active setting like the Eastern Mediterranean, tectonic processes must be considered for palaeogeographic reconstructions. In several palaeogeographic reconstructions the assumed source rocks for the Talea Ori group in the Sakarya Zone, as well as the Karaburun sediments, restore far to the east, which would imply that a wide ocean separating Gondwana and Eurasia was located to the south, since the Palaeotethys opened up to the east (e.g. Stampfli *et al.* 2003; Stampfli & Kozur, 2006; Löwen *et al.* 2017). Eastward terrane displacement by strike-slip faults (possibly also combined with southward subduction) was suggested to provide an alternative in which the Karaburun sediments and Sakarya Zone were located more in the west during Permian times and only later, due to reassembly of Pangaea, were transported hundreds of km to the east (Robertson & Ustaömer, 2009). In such a palaeogeographic situation, the Sakarya Zone should have been located more in the western Palaeotethys closer to the northern margin of Gondwana (e.g. Şengör *et al.* 1984; Golonka *et al.* 2006). Considering a position of the source areas for the siliciclastic metasediments of the lower Talea Ori group in the west, where the Palaeotethys had much smaller N–S extent, sediment transport to a location at the northern margin of Gondwana might be more likely (Fig. 15c).

5.c.4. Deposition of the Talea Ori group north of the PQ s.str.

Based on the zircon spectra with a high amount of euhedral Variscan-aged zircons, Zulauf *et al.* (2016) proposed deposition of the siliciclastic-dominated lower base of the Talea Ori group, the Bali formation, at the southern active margin of Eurasia, which would be in accordance with the new zircon age spectra pointing to the Sakarya Zone as a source. A palaeogeographic origin of the Talea Ori group to the north of the PQ s.str. (Fig. 15d), however, contradicts the association of the Talea Ori group with the Plattenkalk unit, which restores to the northern margin of Gondwana (Baud *et al.* 1993; Marcoux & Baud, 1995; Dornsiepen *et al.* 2001; Stampfli *et al.* 2003; Robertson, 2006, 2012). The main argument for the general association is that the lithofacies of the upper Talea Ori group closely resembles the lithofacies of the Plattenkalk unit at other locations on Crete and the Peloponnesus, indicating a similar palaeogeographic environment (e.g. Creutzburg & Seidel, 1975; Hall & Audley-Charles, 1983; Bonneau, 1984; Jacobshagen *et al.* 1986; Krahl *et al.* 1988; Soujon *et al.* 1998; Krahl & Kauffmann, 2004; Kock *et al.* 2007; Robertson, 2012). The sequence of stromatolitic dolomite marbles (Mavri formation) overlain by a sequence of platy marbles interlayered with chert (Aloides formation) that are interrupted by phyllitic layers (Gigilos beds; Fytrolakis, 1972, 1980) is found in the Lefka Ori as in the Talea Ori (e.g. Krahl *et al.* 1988; Soujon *et al.* 1998). The sedimentary succession – with carbonate breccias at the base and platy marbles that are increasingly interlayered with chert towards the stratigraphic top – indicate subsidence and collapse of the carbonate platform in the Late Triassic / Liassic, which is consistent with a pulse of rifting at the northern margin of Gondwana during the Late Triassic (e.g. Robertson, 2006).

Yet, the siliciclastic lower Talea Ori group, the Sisses, Fodele and Bali formations, are not exposed in any other outcrop of the Plattenkalk unit on Crete and the Peloponnesus. Also, the younger pelitic parts of the Plattenkalk unit, the Kalavros beds, are missing in the Talea Ori (e.g. Epting *et al.* 1972; Hall & Audley-Charles, 1983; Papanikolaou & Vassilakis, 2010). On the Peloponnesus, the siliciclastic base of the platy marbles and cherts of the Taygetos mountains is lithologically different to that of the Talea Ori group (Kowalczyk & Dittmar, 1991) and similar to the phyllites and quartzites of western Crete (Robertson, 2012). The Plattenkalk unit and continuous siliciclastic sediment sequences of Carboniferous to Triassic age, such as the phyllites and quartzites of central and western Crete, are typical pelagic sequences of the southern Palaeotethys (e.g. Krahl *et al.* 1983; Kozur & Krahl, 1987; Baud *et al.* 1993; Marcoux & Baud, 1995; Dornsiepen *et al.* 2001; Stampfli *et al.* 2003; Robertson, 2006, 2012; Stampfli & Kozur, 2006). In contrast to the pelagic setting of the Plattenkalk unit, the sedimentary sequence of the lower Talea Ori group can be interpreted as a tectonically unstable shallow-marine setting with terrigenous influx (Epting *et al.* 1972; Kuss & Thorbecke, 1974; König & Kuss, 1980; Robertson, 2006). Therefore, the lower Talea Ori group would be compatible with deposition in a shallow marine environment as is assumed for the Eurasian shelf. The Aloides formation of the upper Talea Ori group, comprising platy marbles with chert commonly also described as Plattenkalk, are usually interpreted as a pelagic sequence (e.g. Epting *et al.* 1972; Krahl *et al.* 1988; Krahl & Kauffmann, 2004; Robertson, 2006, 2012), but in contrast a shallow marine facies was inferred for the similar platy marbles with chert of the Ida Ori based on lithistid demosponges (e.g. Manutsoglu *et al.* 1995b; Soujon *et al.* 1998). Even a pelagic setting of the Aloides formation may be reconciled with a palaeogeographic

origin in the northern Palaeotethys, since smaller pelagic carbonate platforms existed also at the Eurasian continental margin during the Middle to Late Jurassic (e.g. Haas *et al.* 2011).

Furthermore, the structural position of the Plattenkalk unit and the Talea Ori group that structurally underlie the PQ s.str. must be taken into account. The Plattenkalk unit forms the lowermost unit of the Cretan nappe pile and is commonly described as ‘parautochthonous’ (e.g. Creutzburg & Seidel, 1975; Hall & Audley-Charles, 1983; Bonneau, 1984; Jacobshagen *et al.* 1986; Krahl & Kauffmann, 2004). Assuming a nappe stacking process during N–S compression in the course of the Alpine orogeny with nappe transport from north to south and the southern nappes at the base and the more northern nappes at the top, the structural position is consistent with a palaeogeographic origin of the Plattenkalk unit to the south of the PQ s.str. (e.g. Dornsiepen *et al.* 2001; Robertson, 2006). The parautochthonous character of the Talea Ori group, however, is obsolete, because the geological record reveals a similar Alpine deformation and metamorphic history as the PQ s.str., evidencing burial to 30 km depth and rapid exhumation (e.g. Seidel, 1978; Seidel *et al.* 1982; Theye, 1988; Theye *et al.* 1992; Rahl *et al.* 2005; Seybold *et al.* 2019). A palaeogeographic origin to the north of the PQ s.str. might be reconciled with the structural position below the PQ s.str., assuming the variety of tectonic processes that are possible during subduction. For example, the Talea Ori group located to the north of the PQ s.str. may have entered the subduction channel first, and both units were superimposed on each other during early exhumation, consistent with field observations of an extensional shear zone contact between both units (Seybold *et al.* 2019).

In summary, it cannot be excluded that the Talea Ori group was deposited further north than the PQ s.str. and thus might not be associated with the Plattenkalk unit (Fig. 15d). However, since the lithologies of the upper Talea Ori group closely resemble the Plattenkalk unit in other outcrops of Crete, we judge this alternative to be not very likely. The three alternatives in which the Talea Ori group restores to the northern margin of Gondwana do not exclude each other and combinations might be considered, i.e. sediment transport from different source areas in combination with terrane displacement. The suggested alternatives taking zircon data, structural and lithological arguments into account have further to be tested. For example, more lithological and tectonic constraints as well as new $\varepsilon_{\text{Hf}(t)}$ data may help to distinguish if the Sakarya Zone is indeed a probable source region for the siliciclastic metasediments of the Talea Ori group.

6. Conclusions

- The siliciclastic sediments of the Bali, Fodele and Sisses formations of the lower Talea Ori group are derived mainly from two different source areas: (1) a distal source, characterized by zircon age spectra with Early Palaeozoic and Early Carboniferous age peaks together with a high amount of Neoproterozoic zircons, a Mesoproterozoic age gap and a low amount of Palaeoproterozoic- and Archaean-aged zircons; (2) a proximal source characterized by dominant Late Variscan zircon ages and euhedral zircons (Kock *et al.* 2007; Zulauf *et al.* 2016).
- During the Late Carboniferous / Early Permian, sediments from the proximal Variscan source were delivered and deposited on a shelf slope, possibly close to a pelagic realm (black metachert). Still during the Late Carboniferous / Early Permian, there was a change to recycled Early Palaeozoic to Early Carboniferous (>325 Ma) zircons together with a high amount of recycled zircons with U–Pb ages indicating East Gondwana affinity (70 %),

pointing to a distal source area, the hinterland of the shelf. The U–Pb age spectrum of detrital zircons typical for the distal hinterland was prolongating 40 Ma until the Olenekian.

- Based on the detrital zircons with Neoproterozoic ages, consistent with an East Gondwana derivation, and Cambrian to Devonian and Variscan ages, the Sakarya Zone is one possible distal sediment source for the lower Talea Ori group, which was located in the hinterland of the shelf at the southern active margin of Eurasia. Another possibility would be westerly sources; however, these sources are not yet specified. Despite their Variscan plutons and metamorphism, the West African-related terranes (Morocco, Algerian), the Amazonian and the Avalonian/Baltic terranes (Pelagonian terrane) can be excluded as source areas, because their metamorphic and/or detrital age patterns are not compatible with the Mesoproterozoic age gap combined with a high amount of Tonian/Stenian zircons, which are both significant for the lower Talea Ori group detrital zircon age patterns.
- A palaeogeographic position of the Talea Ori group at the northern margin of Gondwana, as is so far assumed, can be reconciled with the zircon data assuming a combination of different alternatives. These include sediment transport from still unspecified westerly sources in the Aegean region and central Europe as well as the Sakarya Zone at the southern active margin of Eurasia as important source area. Long-distance sediment transport through the Palaeotethys from the Sakarya Zone and eastward terrane displacement allowing for shorter sediment transport distances are suggested to bring sediment to the palaeogeographic origin of the Talea Ori group at the northern margin of Gondwana. The alternative that the Talea Ori group deposited north of the PQ s.str. is not excluded, but in this case the association of the Talea Ori group with the Plattenkalk unit must be reconsidered in combination with lithological, structural and biofacial investigations.

Detrital zircon age spectra in combination with lithological and structural observations are a powerful tool to characterize provenance and to constrain the palaeogeographic origin of the metamorphic rocks in the Talea Ori, an important area for palaeotectonic reconstruction in the complicated Eastern Mediterranean region.

Supplementary Material. To view supplementary material for this article, please visit <https://doi.org/10.1017/S0016756819001365>

Acknowledgements. This study was funded by the Deutsche Forschungsgemeinschaft (DFG Grant no. TR534/5-1). Gernold Zulauf and Otto Förster are gratefully acknowledged for discussions. We thank Linda Marko for help with isotopic analyses and Ferdinand Kirchner for help with sample preparation. We are grateful to Namvar Jahanmehr for preparation of thin-sections. Vasileios Chatzaras, Alastair Robertson and one anonymous reviewer are gratefully acknowledged for constructive reviews that greatly improved the quality of the manuscript.

Declaration of Interest. None.

References

- Abdelsalam MG, Liégeois J-P and Stern RJ (2002). The Saharan metacraton. *Journal of African Earth Sciences* **34**, 119–36.
- Alexopoulos A, Hang H and Krahl J (2000). First Nummulites from the “Plattenkalk” sequence in the Lefka Ori, west Crete. *Annales Géologiques des Pays Helléniques* **38**, 117–21.

- Avigad D, Gerdes A, Morag N and Bechstädt T** (2012). Coupled U–Pb–Hf of detrital zircons of Cambrian sandstones from Morocco and Sardinia: implications for provenance and Precambrian crustal evolution of North Africa. *Gondwana Research* **21**, 690–703.
- Avigad D, Kolodner K, McWilliams M, Persing H and Weissbrod T** (2003). Origin of northern Gondwana Cambrian sandstone revealed by detrital zircon SHRIMP dating. *Geology* **31**, 227–30.
- Aysal N, Öngen S, Peytcheva I and Keskin M** (2012a). Origin and evolution of the Havran Unit, Western Sakarya basement (NW Turkey): new LA-ICP-MS U–Pb dating of the metasedimentary-metagranitic rocks and possible affiliation to Avalonian microcontinent. *Geodinamica Acta* **25**, 226–47.
- Aysal N, Ustaömer T, Öngen S, Keskin M, Köksal S, Peytcheva I and Fanning M** (2012b). Origin of the early-middle Devonian magmatism in the Sakarya zone, NW Turkey: geochronology, geochemistry and isotope systematics. *Journal of Asian Earth Sciences* **45**, 201–22. doi: [10.1016/j.jseas.2011.10.011](https://doi.org/10.1016/j.jseas.2011.10.011).
- Balen D, Horvath P, Tomljenović B, Finger F, Humer B, Pamic J and Arkai P** (2006). A record of pre-Variscan Barrovian regional metamorphism in the eastern part of the Slavonian Mountains (NE Croatia). *Mineralogy and Petrology* **87**, 143–62.
- Baud A, Marcoux J, Guiraud R, Ricou L and Gaetani M** (1993). *Late Murgabian (266 to 264 Ma) Paleoenvironment Map, Explanatory Notes*. Paris: Gauthier-Villars, 9–20.
- Bea F, Montero P, Talavera C, Abu Anbar M, Scarrow JH, Molina JF and Moreno JA** (2010). The palaeogeographic position of central Iberia in Gondwana during the Ordovician: evidence from zircon chronology and Nd isotopes. *Terra Nova* **22**, 341–6.
- Be'eri-Shlevin Y, Eyal M, Eyal Y, Whitehouse MJ and Litvinovsky B** (2012). The Sa'al volcanosedimentary complex (Sinai, Egypt): a latest Mesoproterozoic volcanic arc in the northern Arabian Nubian Shield. *Geology* **40**, 403–6.
- Be'eri-Shlevin Y, Katzir Y and Whitehouse M** (2009a). Post-collisional tectonomagmatic evolution in the northern Arabian–Nubian Shield: time constraints from ion-probe U–Pb dating of zircon. *Journal of the Geological Society* **166**, 71–85.
- Be'eri-Shlevin Y, Katzir Y, Whitehouse MJ and Kleinhanns IC** (2009b). Contribution of pre Pan-African crust to formation of the Arabian Nubian Shield: new secondary ionization mass spectrometry U–Pb and O studies of zircon. *Geology* **37**, 899–902.
- Bonneau M** (1984). Correlation of the hellenide nappes in the south-east Aegean and their tectonic reconstruction. In the *Geological Evolution of the Eastern Mediterranean* (eds JE Dixon and AHF Robertson), pp. 517–27. Geological Society of London, Special Publication no. 17.
- Bowes D and Aftalion M** (1991). U–Pb zircon isotopic evidence for Early Ordovician and Late Proterozoic units in the Mariánské Lázně complex, central-European Hercynides. *Neues Jahrbuch für Mineralogie-Monatshefte* **7**, 315–26.
- Brätz H** (2000). *Radiometrische Altersdatierungen und geochemische Untersuchungen von Orthogneisen, Graniten und Granitporphyren aus dem Ruhlaer Kristallin, mitteldeutsche Kristallinzone*. Thesis, Julius-Maximilians-Universität Würzburg, Würzburg, Germany. Published thesis.
- Candan O, Akal C, Koralay OE, Okay AI, Oberhänsli R, Prelević D and Mertz-Kraus R** (2016). Carboniferous granites on the northern margin of Gondwana, Anatolide-Tauride block, Turkey: evidence for southward subduction of paleotethys. *Tectonophysics* **683**, 349–66.
- Champod E and Vandelli A** (2010). *Stampfli field course. Tectonostratigraphy and plate tectonics of Crete*. Lausanne: Université de Lausanne.
- Chatzaras V, Dörr W, Gerdes A, Krahl J, Xypolias P and Zulauf G** (2016). Tracking the late Paleozoic to early Mesozoic margin of northern Gondwana in the Hellenides: paleotectonic constraints from U–Pb detrital zircon ages. *International Journal of Earth Sciences* **105**, 1881–99.
- Chatzaras V, Xypolias P and Doutsos T** (2006). Exhumation of high-pressure rocks under continuous compression: a working hypothesis for the southern Hellenides (central Crete, Greece). *Geological Magazine* **143**, 859–76.
- Crasquin-Soleau S, Vaslet D and Le Nindre YM** (2006). Ostracods of the Permian-Triassic Khuff Formation, Saudi Arabia: palaeoecology and palaeobiogeography. *GeoArabia* **11**, 55–76.
- Creutzburg N and Seidel E** (1975). Zum Stand der Geologie des Präneogens auf Kreta. *Neues Jahrbuch für Geologie und Paläontologie Abhandlungen* **198**, 363–83.
- Da Silva ÍD, Fernández RD, Díez-Montes A, Clavijo EG and Foster DA** (2016). Magmatic evolution in the N-Gondwana margin related to the opening of the Rheic Ocean: evidence from the Upper Parautochthon of the Galicia-Trás-os-Montes Zone and from the Central Iberian Zone (NW Iberian Massif). *International Journal of Earth Sciences* **105**, 1127–51.
- Deckert C, Plank M, Seidel M and Zacher W** (1999). Die metamorphen Decken des Taygetos-Gebirges (Peloponnes) und ihre Korrelation mit den metamorphen Einheiten auf Kreta: Neugliederung, Vergleiche und Denkmodelle. *Zeitschrift der Deutschen Geologischen Gesellschaft* **480**, 133–58.
- Dombrowski A, Okrusch M, Richter P, Henjes-Kunst F, Höhndorf A and Kröner A** (1995). Orthogneisses in the Spessart Crystalline Complex, north-west Bavaria: Silurian granitoid magmatism at an active continental margin. *Geologische Rundschau* **84**, 399–411.
- Dornsiepen UF and Manutsoğlu E** (1994). Zur Gliederung der Phyllit-Decke Kretas und des Peloponnes. *Zeitschrift der Deutschen Geologischen Gesellschaft* **145**, 286–304.
- Dornsiepen UF, Manutsoğlu E and Mertmann D** (2001). Permian-Triassic palaeogeography of the external Hellenides. *Palaeogeography, Palaeoclimatology, Palaeoecology* **172**, 327–38.
- Dörr W, Fiala J, Vejnar Z and Zulauf G** (1998). U–Pb zircon ages and structural development of metagranitoids of the Teplá crystalline complex: evidence for pervasive Cambrian plutonism within the Bohemian massif (Czech Republic). *Geologische Rundschau* **87**, 135–49.
- Dörr W, Zulauf G, Gerdes A, Lahaye Y and Kowalczyk G** (2015). A hidden Tonian basement in the Eastern Mediterranean: age constraints from U–Pb data of magmatic and detrital zircons of the External Hellenides (Crete and Peloponnesus). *Precambrian Research* **258**, 83–108. doi: [10.1016/j.precambres.2014.12.015](https://doi.org/10.1016/j.precambres.2014.12.015).
- Drost K, Gerdes A, Jeffries T, Linnemann U and Storey C** (2011). Provenance of Neoproterozoic and early Paleozoic siliciclastic rocks of the Teplá-Barrandian unit (Bohemian Massif): evidence from U–Pb detrital zircon ages. *Gondwana Research* **19**, 213–31.
- Engel M and Reischmann T** (1998). Single zircon geochronology of orthogneisses from Paros, Greece. *Bulletin of the Geological Society of Greece* **32**, 91–9.
- Engel M and Reischmann T** (1999). Geochronology of the pre-alpine basement of the central Cyclades, Greece. In *European Union of Geosciences 10, Journal of Conference Abstracts* **4**, 806. Strasbourg: European Union of Geosciences.
- Epting M, Kudrass H, Leppig U and Schäfer A** (1972). Geologie der Talea Ori/Kreta. *Neues Jahrbuch für Geologie und Paläontologie, Abhandlungen* **141**, 259–85.
- Frei D and Gerdes A** (2009). Precise and accurate in situ U–Pb dating of zircon with high sample throughput by automated LA-SF-ICP-MS. *Chemical Geology* **261**, 261–70.
- Friedl G, Finger F, Paquette J-L, von Quadt A, McNaughton NJ and Fletcher IR** (2004). Pre-Variscan geological events in the Austrian part of the Bohemian Massif deduced from U–Pb zircon ages. *International Journal of Earth Sciences* **93**, 802–23.
- Fytrolakis N** (1972). Die Einwirkung gewisser orogener Bewegungen und die Gipsbildung in Ostkreta (Prov. Sitia). *Neues Jahrbuch für Geologie und Paläontologie, Abhandlungen* **9**, 81–100.
- Fytrolakis N** (1980). *Der Geologische Bau von Kreta. Probleme, Beobachtungen und Ergebnisse*. Habil thesis, Technical University of Athens, Athens, Greece. 146 pp. Published thesis.
- Golonka J, Gahagan L, Krobicki M, Marko F, Oszczypko N and Slaczka A** (2006). Plate-tectonic evolution and paleogeography of the circum-Carpathian region. In *The Carpathians and Their Foreland: Geology and Hydrocarbon Resources* (eds J Golonka and F Picha), pp. 11–46. American Association of Petroleum Geologists, Memoir 84.
- Göncüoğlu MC, Capkinoğlu Ş, Gürsu S, Noble P, Turhan N, Tekin UK, Okuyucu C and Göncüoğlu Y** (2007). The Mississippian in the Central and Eastern Taurides (Turkey): constraints on the tectonic setting of the Tauride-Anatolide Platform. *Geologica Carpathica* **58**, 427–42.

- Haas J, Kovács S, Gawlick H-J, Grădinaru E, Karamata S, Sudar M, Péro C, Mello J, Polák M, Ogorelec B and Buser S (2011). Jurassic evolution of the tectonostratigraphic units of the circum-Pannonian region. *Jahrbuch der Geologischen Bundesanstalt, Wien* **151**, 281–354.
- Hall R and Audley-Charles M (1983). The structure and regional significance of the Talea Ori, Crete. *Journal of Structural Geology* **5**, 167–79.
- Himmerkus F, Anders B, Reischmann T and Kostopoulos D (2007). Gondwana-derived terranes in the northern Hellenides. *Memoirs of the Geological Society of America* **200**, 379–90.
- Himmerkus F, Reischmann T and Kostopoulos D (2006). Late Proterozoic and Silurian basement units within the Serbo-Macedonian massif, northern Greece: the significance of terrane accretion in the Hellenides. In *Tectonic Development of the Eastern Mediterranean Region* (eds AHF Robertson and D Mountrakis), pp. 35–50. Geological Society of London, Special Publication no. 260.
- Himmerkus F, Reischmann T and Kostopoulos D (2009). Serbo-Macedonian revisited: a Silurian basement terrane from northern Gondwana in the Internal Hellenides, Greece. *Tectonophysics* **473**, 20–35.
- Jackson SE, Pearson NJ, Griffin WL and Belousova EA (2004). The application of laser ablation inductively coupled plasma-mass spectrometry to in situ U–Pb zircon geochronology. *Chemical Geology* **211**, 47–69.
- Jacobshagen V, Dürr S, Kockel F, Kopp K, Kowalczyk G, Berckhemer H and Büttner D (1978). *Structure and geodynamic evolution of the Aegean region. In Alps, Apennines, Hellenides* (eds H Cloos, D Roeder and K Schmidt), pp. 455–77. IUGG Report 38. Stuttgart: Schweizerbart.
- Jacobshagen V, Dürr S, Kockel F, Makris J, Dornsiepen UF, Giese P and Wallbrecher E (1986). *Geologie von Griechenland. Beiträge zur regionalen Geologie der Erde, Band 19*. Berlin–Stuttgart: Borntraeger, 363 pp.
- Johnson PR and Woldehaimanot B (2003). Development of the Arabian-Nubian Shield: perspectives on accretion and deformation in the northern East African Orogen and the assembly of Gondwana. 289–325. Geological Society of London, Special Publication no. 206.
- Katsivriaris N *et al.* (2008). Geological map of Anoyia, Crete, 1:50000, 1st edn. Athens: Geological Survey of Greece.
- Klein T, Craddock J and Zulauf G (2013). Constraints on the geodynamical evolution of Crete: insights from illite crystallinity, Raman spectroscopy and calcite twinning above and below the ‘Cretan detachment’. *International Journal of Earth Sciences* **102**, 139–82.
- Kock S, Martini R, Reischmann T and Stampfli G (2007). Detrital zircon and micropalaeontological ages as new constraints for the lowermost tectonic unit (Talea Ori unit) of Crete, Greece. *Palaeogeography, Palaeoclimatology, Palaeoecology* **243**, 307–21.
- Koglin N, Zeh A, Franz G, Schüssler U, Glodny J, Gerdes A and Brätz H (2018). From Cadomian magmatic arc to Rheic ocean closure: the geochronological-geochemical record of nappe protoliths of the Münchberg Massif, NE Bavaria (Germany). *Gondwana Research* **55**, 135–52.
- Kolodner K, Avigad D, McWilliams M, Wooden J, Weissbrod T and Feinstein S (2006). Provenance of north Gondwana Cambrian–Ordovician sandstone: U–Pb SHRIMP dating of detrital zircons from Israel and Jordan. *Geological Magazine* **143**, 367–91.
- König H and Kuss S (1980). Neue Daten zur Biostratigraphie des permotriatischen Autochthons der Insel Kreta (Griechenland). *Neues Jahrbuch für Geologie und Paläontologie, Monatshefte* **9**, 525–40.
- Kowalczyk G and Dittmar U (1991). The metamorphics underlying the Plattenkalk carbonates in the Taygetos mts (Southern Peloponnese). *Bulletin of the Geological Society of Greece* **25**, 455–67.
- Kozur H and Krahl J (1987). Erster Nachweis von Radiolarien im tethyalen Perm Europas. *Neues Jahrbuch für Geologie und Paläontologie, Abhandlungen* **174**, 357–72.
- Kozur H and Pjatakova M (1976). Die Conodontenart anchignathodus parvus n. sp., eine wichtige Leitform der basalen Trias. *Koninklijk Nederlands Akademie van Wetenschappen-Amsterdam Series B* **79**, 123–8.
- Krahl J and Kauffmann G (2004). New aspects for a palinspastic model of the External Hellenides on Crete. In *Proceedings of the 5th International Symposium on Eastern Mediterranean Geology, 14–20 April 2004, Thessaloniki, Greece 1* (eds AA Chatzipetros and SB Pavlides), pp. 19–22.
- Krahl J, Kauffmann G, Kozur H, Richter D, Förster O and Heinritz F (1983). Neue Daten zur Biostratigraphie und zur tektonischen Lagerung der Phyllit-Gruppe und der Trypali-Gruppe auf der Insel Kreta (Griechenland). *Geologische Rundschau* **72**, 1147–66.
- Krahl J, Kauffmann G, Richter D, Kozur H, Möller I, Förster O, Heinritz F and Dornsiepen U (1986). Neue Fossilfunde in der Phyllit-Gruppe Ostkretas (Griechenland). *Zeitschrift der deutschen geologischen Gesellschaft* **137**, 523–36.
- Krahl J, Richter D, Förster O, Kozur H and Hall R (1988). Zur Stellung der Talea Ori im Bau des kretischen Deckenstapels (Griechenland). *Zeitschrift der deutschen geologischen Gesellschaft* **139**, 191–227.
- Kröner A, Jaekel P, Hegner E and Opletal M (2001). Single zircon ages and whole-rock Nd isotopic systematics of early Palaeozoic granitoid gneisses from the Czech and Polish Sudetes (Jizerské hory, Krkonoše Mountains and Orlice-Sněžník Complex). *International Journal of Earth Sciences* **90**, 304–24.
- Kröner A and Stern R (2005). AFRICA| Pan-African orogeny. In *Encyclopedia of Geology* **1**, pp. 1–12. Amsterdam, Elsevier.
- Kuss S (1963). Erster Nachweis von permischen Fusulinen auf der Insel Kreta. *Praktika tēs Akadēmias Athēnōn* **38**, 431–6.
- Kuss S (1973). Neue Fusulinenfunde in den Talea Ori/Kreta (Griechenland). *Berichte der Naturforschenden Gesellschaft zu Freiburg im Breisgau* **63**, 73–9.
- Kuss S (1982). Ein erster Ammonitenfund aus der Plattenkalk-Formation der Insel Kreta/Griechenland. *Bericht der Naturforschenden Gesellschaft zu Freiburg im Breisgau* **71/72**, 35–8.
- Kuss S and Thorbecke G (1974). Die präneogenen Gesteine der Insel Kreta und ihre Korrelierbarkeit im ägäischen Raum. *Berichte der Naturforschenden-Gesellschaft zu Freiburg im Breisgau* **64**, 39–75.
- Küster D, Liégeois J-P, Matukov D, Sergeev S and Lucassen F (2008). Zircon geochronology and Sr, Nd, Pb isotope geochemistry of granitoids from Bayuda Desert and Sabaloka (Sudan): evidence for a Bayudian event (920–900 Ma) preceding the Pan-African orogenic cycle (860–590 Ma) at the eastern boundary of the Saharan Metacraton. *Precambrian Research* **164**, 16–39.
- Kydonakis K, Kostopoulos D, Poujol M, Brun J-P, Papanikolaou D and Paquette J-L (2014). The dispersal of the Gondwana Super-fan system in the Eastern Mediterranean: new insights from detrital zircon geochronology. *Gondwana Research* **25**, 1230–41.
- Linnemann U, Gerdes A, Drost K and Buschmann B (2007). The continuum between Cadomian orogenesis and opening of the Rheic Ocean: constraints from LA-ICP-MS U–Pb zircon dating and analysis of plate-tectonic setting (Saxo-Thuringian zone, northeastern Bohemian Massif, Germany). *Geological Society of America Special Paper*, **423**, 61–96.
- Linnemann U, McNaughton NJ, Romer RL, Gehmlich M, Drost K and Tonk C (2004). West African provenance for Saxo-Thuringia (Bohemian Massif): did Armorica ever leave pre-Pangean Gondwana? – U/Pb-SHRIMP zircon evidence and the Nd-isotopic record. *International Journal of Earth Sciences* **93**, 683–705.
- Linnemann U, Ouzegane K, Drareni A, Hofmann M, Becker S, Gärtner A and Sagawe A (2011). Sands of West Gondwana: an archive of secular magmatism and plate interactions: a case study from the Cambro-Ordovician section of the Tassili Ouan Ahaggar (Algerian Sahara) using U–Pb–LA-ICP-MS detrital zircon ages. *Lithos* **123**, 188–203.
- Linnemann U, Pereira F, Jeffries TE, Drost K and Gerdes A (2008). The Cadomian Orogeny and the opening of the Rheic Ocean: the diachrony of geotectonic processes constrained by LA-ICP-MS U–Pb zircon dating (Ossa-Morena and Saxo-Thuringian Zones, Iberian and Bohemian Massifs). *Tectonophysics* **461**, 21–43.
- Lippolt HJ (1986). Nachweis altpaläozoischer Primäralter (Rb–Sr) und karbonischer Abkühlungsalter (K–Ar) der Muskovit-Biotit-Gneise des Spessarts und der Biotit-Gneise des Böllsteiner Odenwaldes. *Geologische Rundschau* **75**, 569–83.
- Löwen K, Bröcker M and Berndt J (2015). Depositional ages of clastic meta-sediments from Samos and Syros, Greece: results of a detrital zircon study. *International Journal of Earth Sciences* **104**, 205–20.
- Löwen K, Meinhold G, Güngör T and Berndt J (2017). Palaeotethys-related sediments of the Karaburun Peninsula, western Turkey: constraints on provenance and stratigraphy from detrital zircon geochronology. *International Journal of Earth Sciences* **106**, 2771–96.
- Ludwig K (2001). Users manual for isoplot/Ex (rev. 2.49): a geochronological toolkit for Microsoft Excel. *Berkeley Geochronology Center, Special Publication* **1**, 55 pp.

- Manutsoglu E, Mertmann D, Soujon A, Dornsiepen U and Jacobshagen V** (1995a). Zur Nomenklatur der Metamorphite auf der Insel Kreta, Griechenland. *Berliner Geowissenschaften Abhandlungen* **16**, 579–88.
- Manutsoglu E, Soujon A, Reitner J and Dornsiepen UF** (1995b). Relikte lithistider Demospongiae aus der metamorphen Plattenkalk-Serie der Insel Kreta (Griechenland) und ihre paläobathymetrische Bedeutung. *Neues Jahrbuch für Geologie und Paläontologie-Monatshefte* **4**, 235–47.
- Marcoux J and Baud A** (1995). Late Permian to Late Triassic, Tethyan paleoenvironments. In *The Tethys Ocean* (eds AEM Nairn, LE Ricou, B Vrielynck and J Dercourt), pp. 153–90. Boston: Springer.
- Marsellos A, Foster DA, Kamenov G and Kyriakopoulos K** (2012). Detrital zircon U-Pb data from the Hellenic South Aegean belts: constraints on the age and source of the South Aegean basement. *Journal of the Virtual Explorer* **42**, 1–12.
- Meert JG and Van der Voo R** (1997). The assembly of Gondwana 800–550 Ma. *Journal of Geodynamics* **23**, 223–35.
- Meinhold G, Kostopoulos D, Frei D, Himmerkus F and Reischmann T** (2010). U-Pb LA-SF-ICP-MS zircon geochronology of the Serbo-Macedonian Massif, Greece: palaeotectonic constraints for Gondwana-derived terranes in the Eastern Mediterranean. *International Journal of Earth Sciences* **99**, 813–32.
- Meinhold G, Morton AC, Fanning CM, Frei D, Howard JP, Phillips RJ, Strogon D and Whitham AG** (2011). Evidence from detrital zircons for recycling of Mesoproterozoic and Neoproterozoic crust recorded in Paleozoic and Mesozoic sandstones of Southern Libya. *Earth and Planetary Science Letters* **312**, 164–75.
- Meinhold G, Reischmann T, Kostopoulos D, Lehnert O, Matukov D and Sergeev S** (2008). Provenance of sediments during subduction of Palaeotethys: detrital zircon ages and olistolith analysis in Palaeozoic sediments from Chios Island, Greece. *Palaeogeography, Palaeoclimatology, Palaeoecology* **263**, 71–91.
- Moix P, Beccalotto L, Kozur HW, Hochard C, Rosselet F and Stampfli GM** (2008). A new classification of the Turkish terranes and sutures and its implication for the paleotectonic history of the region. *Tectonophysics* **451**, 7–39.
- Montero P, Bea F, Zinger T, Searrow J, Molina J and Whitehouse M** (2004). 55 million years of continuous anatexis in Central Iberia: single-zircon dating of the Pena Negra Complex. *Journal of the Geological Society* **161**, 255–63.
- Morag N, Avigad D, Gerdes A, Belousova E and Harlavan Y** (2011a). Crustal evolution and recycling in the northern Arabian-Nubian Shield: new perspectives from zircon Lu-Hf and U-Pb systematics. *Precambrian Research* **186**, 101–16. doi: 10.1016/j.precamres.2011.01.004.
- Morag N, Avigad D, Gerdes A, Belousova E and Harlavan Y** (2011b). Long-distance transport of North Gondwana Cambro-Ordovician sandstones: evidence from detrital zircon Hf isotopic composition. *Mineralogical Magazine* **75**, 1497.
- Murphy JB, Fernández-Suárez J, Jeffries T and Strachan R** (2004a). U-Pb (LA-ICP-MS) dating of detrital zircons from Cambrian clastic rocks in Avalonia: erosion of a Neoproterozoic arc along the northern Gondwanan margin. *Journal of the Geological Society* **161**, 243–54.
- Murphy JB, Fernández-Suárez J and Jeffries TE** (2004b). Litho-geochemical and Sm-Nd and U-Pb isotope data from the Silurian-Lower Devonian Arisaig group clastic rocks, Avalon terrane, Nova Scotia: a record of terrane accretion in the Appalachian-Caledonide orogen. *Geological Society of America Bulletin* **116**, 1183–201.
- Nance RD, Murphy JB, Strachan RA, Keppie JD, Gutiérrez-Alonso G, Fernández-Suárez J, Quesada C, Linnemann U, D'lemos R and Pisarevsky SA** (2008). Neoproterozoic-early Palaeozoic tectonostratigraphy and palaeogeography of the peri-Gondwanan terranes: Amazonian v. West African connections. In *The Boundaries of the West African Craton* (eds N Ennih and J-P Liégeois), pp. 345–83. Geological Society of London, Special Publication no. 297.
- Okay A, Satir M, Maluski H, Siyako M, Monie P, Metzger R and Akyüz S** (1996). Paleo- and Neo-Tethyan events in northwestern Turkey: geologic and geochronologic constraints. In *The Tectonic Evolution of Asia* (eds A Yin and TM Harrison), pp. 420–41. Cambridge: Cambridge University Press.
- Okay A, Satir M and Siebel W** (2006). Pre-Alpine Palaeozoic and Mesozoic orogenic events in the Eastern Mediterranean region. *Memoirs of the Geological Society of London* **32**, 389–405.
- Okay AI, Bozkurt E, Satir M, Yiğitbaş E, Crowley QG and Shang CK** (2008a). Defining the southern margin of Avalonia in the Pontides: geochronological data from the Late Proterozoic and Ordovician granitoids from NW Turkey. *Tectonophysics* **461**, 252–64.
- Okay AI, Satir M and Shang CK** (2008b). Ordovician metagranitoid from the Anatolide-Tauride Block, northwest Turkey: geodynamic implications. *Terra Nova* **20**, 280–8.
- Özbey Z, Ustaömer T, Robertson AH and Ustaömer PA** (2013). Tectonic significance of Late Ordovician granitic magmatism and clastic sedimentation on the northern margin of Gondwana (Tavşanlı Zone, NW Turkey). *Journal of the Geological Society* **170**, 159–73.
- Özmen F and Reischmann T** (1999). The age of the Sakarya continent in W Anatolia: implications for the evolution of the Aegean region. In *European Union of Geosciences 10, Journal of Conference Abstracts* **4**, 805. Strasbourg: European Union of Geosciences.
- Pamić J and Jurković I** (2002). Paleozoic tectonostratigraphic units of the northwest and central Dinarides and the adjoining South Tisia. *International Journal of Earth Sciences* **91**, 538–54.
- Papanikolaou D and Vassilakis E** (2010). Thrust faults and extensional detachment faults in Cretan tectonostratigraphy: implications for Middle Miocene extension. *Tectonophysics* **488**, 233–47.
- Rahl JM, Anderson KM, Brandon MT and Fassoulas C** (2005). Raman spectroscopic carbonaceous material thermometry of low-grade metamorphic rocks: calibration and application to tectonic exhumation in Crete, Greece. *Earth and Planetary Science Letters* **240**, 339–54.
- Reischmann T, Anthes G, Jaekel P and Altenberger U** (2001). Age and origin of the Böllsteiner Odenwald. *Mineralogy and Petrology* **72**, 29–44.
- Richter D and Kopp K** (1983). Zur Tektonik der untersten geologischen Stockwerke auf Kreta. *Neues Jahrbuch für Geologie und Paläontologie Abhandlungen* **1983**, 27–46.
- Robertson A** (2006). Sedimentary evidence from the south Mediterranean region (Sicily, Crete, Peloponnese, Evia) used to test alternative models for the regional tectonic setting of Tethys during Late Palaeozoic-Early Mesozoic time. In *Tectonic Development of the Eastern Mediterranean Region* (eds AHF Robertson and D Mountrakis), pp. 91–154. Geological Society of London, Special Publication no. 260.
- Robertson AH** (2012). Late Palaeozoic-Cenozoic tectonic development of Greece and Albania in the context of alternative reconstructions of Tethys in the Eastern Mediterranean region. *International Geology Review* **54**, 373–454.
- Robertson AH and Pickett EA** (2000). Palaeozoic-Early Tertiary Tethyan evolution of mélanges, rift and passive margin units in the Karaburun Peninsula (western Turkey) and Chios island (Greece). In *Tectonics and Magmatism in Turkey and the Surrounding Area* (eds E Bozkurt, JA Winchester and JDA Piper), pp. 43–82. Geological Society of London, Special Publication no. 173.
- Robertson AH and Ustaömer T** (2009). Formation of the Late Palaeozoic Konya complex and comparable units in southern Turkey by subduction-accretion processes: implications for the tectonic development of Tethys in the Eastern Mediterranean region. *Tectonophysics* **473**, 113–48.
- Romano SS, Brix MR, Dörr W, Fiala J, Krenn E, Zulauf G** (2006). The Carboniferous to Jurassic evolution of the pre-Alpine basement of Crete: constraints from radiometric dating of orthogneiss, fission-track dating of zircon and structural/petrological data. In *Tectonic Development of the Eastern Mediterranean Region* (eds AHF Robertson and D Mountrakis). Geological Society London special Publications 260, 69–90.
- Romano SS, Dörr W and Zulauf G** (2004). Cambrian granitoids in pre-Alpine basement of Crete (Greece): evidence from U-Pb dating of zircon. *International Journal of Earth Sciences* **93**, 844–59.
- Schulz B** (2013). Monazite EMP-Th-U-Pb age pattern in Variscan metamorphic units in the Armorican Massif (Brittany, France)[Monazit-Altersmuster (EMS-Th-U-Pb) in den variskischen metamorphen Einheiten des Armorikanischen Massivs (Bretagne, Frankreich)]. *Zeitschrift der Deutschen Gesellschaft für Geowissenschaften* **164**, 313–35.
- Seidel E** (1978). *Zur Petrologie der Phyllit-Quarzit-Serie Kretas*. Thesis, Technische Universität, Braunschweig, Germany. Published Thesis.
- Seidel E, Kreuzer H and Harre W** (1982). A late Oligocene/early Miocene high pressure belt in the external Hellenides. *Geologisches Jahrbuch* **E 23**, 165–206.

- Seidel M, Seidel E and Stöckhert B (2007). Tectono-sedimentary evolution of lower to middle Miocene half-graben basins related to an extensional detachment fault (western Crete, Greece). *Terra Nova* **19**, 39–47.
- Şengör A, Yılmaz Y and Sungurlu O (1984). Tectonics of the Mediterranean Cimmerides: nature and evolution of the western termination of Palaeo-Tethys. In *The Geological Evolution of the Eastern Mediterranean* (eds JE Dixon and AHF Robertson), pp. 77–112. Geological Society of London, Special Publication no. 17.
- Seybold L, Treppmann CA and Janots E (2019). A ductile extensional shear zone at the contact area between HP-LT metamorphic units in the Talea Ori, central Crete, Greece: deformation during early stages of exhumation from peak metamorphic conditions. *International Journal of Earth Sciences* **108**, 213–27. doi: [10.1007/s00531-018-1650-6](https://doi.org/10.1007/s00531-018-1650-6).
- Soujon A, Jacobshagen V and Manutsoglu E (1998). A lithostratigraphic correlation of the Plattenkalk occurrences of Crete (Greece). *Bulletin of the Geological Society of Greece* **32**, 41–8.
- Stacey JT and Kramers J (1975). Approximation of terrestrial lead isotope evolution by a two-stage model. *Earth and Planetary Science Letters* **26**, 207–21.
- Stampfli G, Hochard C, Vérard C and Wilhem C (2013). The formation of Pangea. *Tectonophysics* **593**, 1–19.
- Stampfli GM and Borel G (2002). A plate tectonic model for the Paleozoic and Mesozoic constrained by dynamic plate boundaries and restored synthetic oceanic isochrons. *Earth and Planetary Science Letters* **196**, 17–33.
- Stampfli GM and Kozur HW (2006). Europe from the Variscan to the Alpine cycles. *Memoirs of the Geological Society of London* **32**, 57–82.
- Stampfli GM, Vavassis I, De Bono A, Rosselet F, Matti B and Bellini M (2003). Remnants of the Paleotethys oceanic suture-zone in the western Tethyan area. Stratigraphic and structural evolution on the Late Carboniferous to Triassic continental and marine successions in Tuscany (Italy): regional reports and general correlation. *Bolletino della Società Geologica Italiana, Volume speciale 2*, 1–24.
- Stephan T, Kroner U and Romer RL (2019). The pre-orogenic detrital zircon record of the Peri-Gondwanan crust. *Geological Magazine* **156**, 281–307.
- Stern RJ (1994). Arc assembly and continental collision in the Neoproterozoic East African Orogen: implications for the consolidation of Gondwanaland. *Annual Review of Earth and Planetary Sciences* **22**, 319–51.
- Sunal G (2012). Devonian magmatism in the western Sakarya Zone, Karacabey region, NW Turkey. *Geodinamica Acta* **25**, 183–201.
- Teufel S (1988). Vergleichende U–Pb- und Rb–Sr-Altersbestimmungen an Gesteinen des Übergangsbereiches Saxothuringikum/Moldanubikum, NE–Bayern. *Göttingen Arbeiten zur Geologie und Paläontologie* **35**: 1–87.
- Theye T (1988). *Aufsteigende Hochdruckmetamorphose in Sedimenten der Phyllit-Quarzit-Einheit Kretas und des Peloponnes*. Thesis, Technische Universität, Braunschweig, Germany. Published Thesis.
- Theye T and Seidel E (1991). Petrology of low-grade high-pressure metapelites from the External Hellenides (Crete, Peloponnese): a case study with attention to sodic minerals. *European Journal of Mineralogy* **3**, 343–66.
- Theye T, Seidel E and Vidal O (1992). Carpholite, sudoite, and chloritoid in low-grade high-pressure metapelites from Crete and the Peloponnese, Greece. *European Journal of Mineralogy* **4**, 487–508.
- Thomson SN, Stöckhert B and Brix MR (1998). Thermochronology of the high-pressure metamorphic rocks of Crete, Greece: implications for the speed of tectonic processes. *Geology* **26**, 259–62.
- Thomson SN, Stöckhert B and Brix MR (1999). Miocene high-pressure metamorphic rocks of Crete, Greece: rapid exhumation by buoyant escape. In *Exhumation Processes: Normal Faulting, Ductile Flow and Erosion* (eds U Ring, MT Brandon, GS Lister and SD Willett), pp. 87–107. Geological Society of London, Special Publication no. 154.
- Timmermann H, Dörr W, Krenn E, Finger F and Zulauf G (2006). Conventional and in situ geochronology of the Teplá Crystalline unit, Bohemian Massif: implications for the processes involving monazite formation. *International Journal of Earth Sciences* **95**, 629–47.
- Timmermann H, Štědrá V., Gerdes A, Noble S, Parrish RR and Dörr W. (2004). The problem of dating high-pressure metamorphism: a U–Pb isotope and geochemical study on eclogites and related rocks of the Mariánské Lázně Complex, Czech Republic. *Journal of Petrology* **45**, 1311–38.
- Titorenkova R, Macheva L, Zidarov N, Von Quadt A and Peytcheva I (2003). Metagranites from SW Bulgaria as a part of the Neoproterozoic to Early Paleozoic system in Europe: new insight from zircon typology, U–Pb isotope data and Hf-tracing. *Geophysical Research Abstracts* **5**, 08963.
- Treppmann C, Lenze A and Stöckhert B (2010). Static recrystallization of vein quartz pebbles in a high-pressure low-temperature metamorphic conglomerate. *Journal of Structural Geology* **32**, 202–15.
- Treppmann CA and Seybold L (2019). Deformation at low and high stress-loading rates. *Geoscience Frontiers* **10**, 43–54.
- Ustaömer PA, Ustaömer T and Robertson A (2012). Ion probe U–Pb dating of the Central Sakarya basement: a peri-Gondwana terrane intruded by late Lower Carboniferous subduction/collision-related granitic rocks. *Turkish Journal of Earth Sciences* **21**, 905–32.
- Ustaömer T, Robertson AH, Ustaömer PA, Gerdes A and Peytcheva I (2013). Constraints on Variscan and Cimmerian magmatism and metamorphism in the Pontides (Yusufeli–Artvin area), NE Turkey from U–Pb dating and granite geochemistry. In *Geological Development of the Anatolian Continent and the Easternmost Mediterranean Region* (eds AHF Robertson, O Parlak and UC Ünlügenç), pp. 49–94. Geological Society of London, Special Publication no. 372.
- Ustaömer T, Ustaömer PA, Robertson AH and Gerdes A (2019). U–Pb–Hf isotopic data from detrital zircons in late Carboniferous and Mid-Late Triassic sandstones, and also Carboniferous granites from the Tauride and Anatolide continental units in S Turkey: implications for Tethyan palaeogeography. *International Geology Review* **36**, 1–28.
- Wachendorf H, Gralla G, Koll J and Schulze I (1980). Geodynamik des mitteltetrischen Deckenstapels (nördliches Dikti-Gebirge). *Geotektonische Forschungen* **59**, 1–71.
- Wiedenbeck M, Alle P, Corfu F, Griffin WL, Meier M, Oberli FV, Quadt AV, Roddick JC and Spiegel W (1995). Three natural zircon standards for U–Th–Pb, Lu–Hf, trace element and REE analyses. *Geostandards Newsletter* **19**, 1–23.
- Williams IS, Fiannacca P, Cirrincione R and Pezzino A (2012). Peri-Gondwanan origin and early geodynamic history of NE Sicily: a zircon tale from the basement of the Peloritani Mountains. *Gondwana Research* **22**, 855–65.
- Xypolias P, Chatzaras V, Koukouvelas IK (2007). Strain gradients in zones of ductile thrusting: Insights from the external Hellenides. *Journal of Structural Geology* **29**, 1522–1537.
- Xypolias P, Dörr W and Zulauf G (2006). Late Carboniferous plutonism within the pre-Alpine basement of the External Hellenides (Kithira, Greece): evidence from U–Pb zircon dating. *Journal of the Geological Society* **163**, 539–47.
- Zeh A, Cosca M, Brätz H, Okrusch M and Tichomirowa M (2000). Simultaneous horst-basin formation and magmatism during Late Variscan transtension: evidence from $^{40}\text{Ar}/^{39}\text{Ar}$ and $^{207}\text{Pb}/^{206}\text{Pb}$ geochronology in the Ruhla Crystalline Complex. *International Journal of Earth Sciences* **89**, 52–71.
- Zeh A, Williams IS, Brätz H and Millar IL (2003). Different age response of zircon and monazite during the tectono-metamorphic evolution of a high grade paragneiss from the Ruhla Crystalline Complex, central Germany. *Contributions to Mineralogy and Petrology* **145**, 691–706.
- Zhang Y-C and Wang Y (2018). Permian fusuline biostratigraphy. In *The Permian Timescale* (eds SG Lucas and SZ Shen), pp. 253–88. Geological Society of London, Special Publication no. 450. doi: [10.1144/SP450.14](https://doi.org/10.1144/SP450.14).
- Zlatkin O, Avigad D and Gerdes A (2013). Evolution and provenance of Neoproterozoic basement and Lower Paleozoic siliciclastic cover of the Menderes Massif (western Taurides): coupled U–Pb–Hf zircon isotope geochemistry. *Gondwana Research* **23**, 682–700.
- Zulauf G, Dörr W, Fisher-Spurlock S, Gerdes A, Chatzaras V and Xypolias P (2015). Closure of the Paleotethys in the External Hellenides: constraints from U–Pb ages of magmatic and detrital zircons (Crete). *Gondwana Research* **28**, 642–67.
- Zulauf G, Dörr W, Krahl J, Lahaye Y, Chatzaras V and Xypolias P (2016). U–Pb zircon and biostratigraphic data of high-pressure/low-temperature metamorphic rocks of the Talea Ori: tracking the Paleotethys suture in central Crete, Greece. *International Journal of Earth Sciences* **105**, 1901–22.

- Zulauf G, Dörr W, Marko L and Krahl J** (2018). The late Eo-Cimmerian evolution of the external Hellenides: constraints from microfabrics and U–Pb detrital zircon ages of Upper Triassic (meta) sediments (Crete, Greece). *International Journal of Earth Sciences* **107**, 2859–94. doi: [10.1007/s00531-018-1632-8](https://doi.org/10.1007/s00531-018-1632-8).
- Zulauf G, Klein T, Kowalczyk G, Krahl J and Romano SS** (2008). The Mirsini Syncline of eastern Crete, Greece: a key area for understanding pre-Alpine and Alpine orogeny in the Eastern Mediterranean [Die Mulde von Mirsini in Ostkreta, Griechenland: ein Schlüsselgebiet zum Verständnis präalpiner und alpiner Orogenese im östlichen Mittelmeerraum.]. *Zeitschrift der deutschen Gesellschaft für Geowissenschaften* **159**, 399–414.
- Zulauf G, Romano S, Dörr W and Fiala J** (2007). Crete and the Minoan terranes: age constraints from U–Pb dating of detrital zircons. In *The Evolution of the Rheic Ocean: From Avalonian–Cadomian Active Margin to Alleghenian–Variscan Collision* (eds U Linnemann, RD Nance, P Kraft and G Zulauf), pp. 401–11. Boulder, Colorado: Geological Society of America Special Paper 423.